Designing a Fast Charging System for Lithium-Ion Batteries Based on Double Pulse Method Using Optimized Regulation of Frequency and Duty Cycle

By

AKM Ferdous

17121056

Muyeed Morshed

16321061

Prasis Saha

16321143

Kazi Farhan Reaz

16121103

A thesis submitted to the Department of Electrical and Electronic Engineering of BRAC University, in partial fulfillment of the requirements for the degree of Bachelor of Science in Electrical and Electronic Engineering

Department of Electrical and Electronic Engineering
Brac University
September, 2020

Declaration

We hereby declare that

1. The thesis submitted is our own original work while completing degree at Brac University.
2. The thesis does not contain material previously published or written by a third party, except where this is appropriately cited through full and accurate referencing.
3. The thesis does not contain material which has been accepted, or submitted, for any other degree or diploma at a university or other institution.
4. We have acknowledged all main sources of help.

Student's Full Name & Signature:

AKM Ferdous 17121056	**Muyeed Morshed** 16321061
Prasis Saha 16321143	**Kazi Farhan Reaz** 16121103

Approval

The thesis titled "Designing a Fast Charging System for Lithium-Ion Batteries Based on Double Pulse Method Using Optimized Regulation of Frequency and Duty Cycle" submitted by

1. AKM Ferdous (ID: 17121056)
2. Muyeed Morshed (ID: 16321061)
3. Prasis Saha (ID: 16321143)
4. Kazi Farhan Reaz (ID: 16121103)

Of Summer, 2020 has been accepted as satisfactory in partial fulfillment of the requirement for the degree of Bachelor of Science in Electrical and Electronic Engineering on 1st October, 2020

Examining Committee:

Supervisor:
(Member)

_____

Abu S.M. Mohsin, Ph.D.
Assistant Professor, Department of Electrical and Electronic Engineering
Brac University

Program Coordinator:
(Member)

_____

Abu S.M. Mohsin, Ph.D.
Assistant Professor, Department of Electrical and Electronic Engineering
Brac University

Departmental Head:
(Chair)

_____

Shahidul Islam Khan, Ph.D.
Professor and Chairperson, Department of Electrical and Electronic Engineering
Brac University

Abstract

Considering the high demand for fast charging in recent times, the pulse charging technique has been identified as one of the fast charging techniques for lithium ion cells to efficiently resolve the limitation of long charging time compared to traditional methods. The pulse charging method is usually considered as a single pulse charging method where it requires two periodic charging stages, one for current injection and the other for resting. A variable frequency and duty cycle are implemented during the single pulse charging method to optimize the acceptable current injection focused on polarization properties. This method has previously proven to charge the lithium ion battery in a time span of 56 minutes with a temperature rise of 13 degrees Celsius. Our thesis aims to prove the effects of the single pulse method and improve the mentioned time and temperature by proposing the use of a double pulse charging method which uses a smaller secondary current between the resting periods of the large primary current without forcing down battery capacity limits. This helps in overcoming the loss of time due to the long resting period without causing raise in temperature. In addition, a current limiting technique was implemented on the primary larger current to lower temperature effects. To do so, MATLAB / Simulink was used to design and implement both charging methods and the results of the proposed method were compared with the single pulse charging strategy. Comparative analysis of our results has shown that the proposed method reduces the charging time almost 10 minutes with no temperature rise compared to the single pulse charging system.

Keywords: charging; current; pulse; polarization; DPC; duty-cycle.

Acknowledgement

First of all, we express our deepest gratitude to the Almighty for the good health and welfare that was essential to complete this thesis book. We would like to thank and express sincere appreciation to our thesis advisor Dr. Abu S.M. Mohsin, Assistant Professor of the Department of Electrical and Electronic Engineering at Brac University, for sharing his expertise and for providing an excellent hand in guiding. He convincingly advised and encouraged us to think critically in solving the puzzles of our research and to be professional throughout our thesis work. Without his encouragement and persistent help, the completion of this thesis on time would not have been possible. We like to dedicate our work and express very profound gratitude to our beloved parents who gave us boundless love, continuous mental and financial unfailing support and offered deep insight into the study.

Table of Contents

List of Tables

List of Figures

List of Acronyms

SOC	State of Charge
Li-Ion	Lithium Ion
PWM	Pulse Width Modulation
AH	Ampere Hour
MOSFET	Metal Oxide Semiconductor Field Effect Transistor
LUT	Look Up Table
CCCV	Constant Current, constant voltage
CL	Current Limiter
DPC	Double Pulse Charging
SPC	Single Pulse Charging

Chapter 1: Introduction

1.1 Motivation

The demands for many large battery cell applications, such as electric cars (EVs) and industrial systems installed in another subnet as well as smartphones, portable computers, printers, camcorders and other electrical appliances, have started in recent Times. In our modern era of technology, battery cells play a major role. There are many advantages of the use of battery cells. This increasingly makes the platform used for a broad range of applications. High energy density is one of the big benefits of battery cell technology. Electronic devices like mobile devices, which need to operate longer between charges but also use more power as well as require batteries with a considerably higher power density. In addition, there are various power applications from electric equipment to electric vehicles. A far higher power density of lithium ion batteries is a major advantage. For several rechargeable batteries, the self-discharge rate is a vial problem. In all other lithium-ion cells, there is considerably less self-discharge than other rechargeable cells such as Ni-Cad and NiMH. In the first four hours after the charge, it is normally around 5%, but then it is around 1% or 2% per month. Also it is anticipated that lithium-ion batteries reduce battery weight by 40 % to 50% as well as battery volumes by 20% to 30% and improve performance significantly **[1].** With the growing number of advanced applications around us, storage batteries like lithium-ion provide ample energy to power these electrical appliances efficiently. The proper charging method must be introduced in order to ensure such performance. As a result, these considerations have motivated us to build a charging mechanism so that we can achieve greater efficiency in charging performance both in our residential applications and in the industrial applications around us.

1.2 Why fast charging?

Fast charging is a power supply control mechanism that either allows higher current rates or increases the voltage flow to the battery. With increasing demands to reduce the charging time for battery-based applications, faster charging of high-energy batteries has been intensively sought as the most critical requirement for practical use in future applications. Fast charging is a successful option. This technology makes charging more effective by reducing the time it takes for the battery to supply a sufficient amount of energy to power our electrical appliances. Consumers know the value of quick charging, as fast charging systems are booming in manufacturing plants and distribution centers all over the world.

The perfect battery with high power and energy densities would have a longer life cycle, allowing long-distance transport at a single charge and fast recharge at any temperature. Unfortunately, tradeoffs contribute to the dynamics of the two criteria **[2].** Lithium-ion battery commercial structure prevents the effort to allow faster charging: improving rapid charge capacity at low temperatures generally results in cell durability being compromised. A cell structure that can be regulated to break this trade off and allow for a fast lithium-free charging. The lithium cell also offers an independent, coherent charging practice for the development of battery materials without restrictions of temperature. Using this technique, a lithium cell of 9.5 Ah 170 Wh/ kg can be charged up to 80% of the load even at -50 ° C (beyond the cell operating limit) at 15 minutes **[2].** As ambient temperatures decrease, charging speeds and recommended maximum voltages are usually kept low to boost safety and efficiency. Along with the temperature issue the aging rate for lithium cells also convey a great concern. Generally, the aging rate of lithium cells is increased at 0.5C with lowering temperature between 25°C and 0°C in order to provide the normal constant current / constant Voltage (CC-CV) charging mechanism **[3].** Interestingly, for CC-CV charging at temperature levels from 25 ° C to 60 ° C at 0.5 C there is no accelerated aging. The observed behavior demonstrates lithium deposition

on anodes up to < 25 ° C. Furthermore, the reconstruction of the commercial INR-18650 cells of the anode and cathode into fully cell with an additional electrode **[3].** Furthermore, electrodes assembly in cumulative cells with reference electrode as a model system which test the effect of various temperatures on the electrode polarizations. Lithium plating is the dominant aging mechanism of T < 25°C, while cathodes degenerative of T > 25°C **[4].** Due to a broad range of electrode compositions, combined with other factors like the loading of electrodes, porosity and electrolytes, our work provides new insights into limiting electrodes, especially for extremely fast charging applications, in various Li-ion batteries **[5].** Moreover, the performance of high-speed charge systems is often heavily dependent on the temperature and the conversion efficiencies of 50 kW chargers have increased up to 93% and operation levels to 39% at 25°C and -25°C respectively **[6].** The degree of this temperature-dependency differs between the loader models, some of which are still capable of maintaining around 70 per cent efficiencies at -25°C and others that do not work at all **[6].**

Fast chargers may help eliminate potential and real obstacles to the selection, making our electrical appliances more favorable. At the existing market, there is a critical need for the support to promote the growth of fast-charging networks. Therefore, we have opted for a fast charging mechanism rather than a conventional charging mechanism.

1.3 Applications of battery

Industrial battery technology discusses all devices and batteries and explores the related science and technical aspects. Presenting large batteries for stationary uses, e.g. energy storage, as well as electric vehicle batteries or other equipment. Both in conjunction with satellites and space flights, the essential aerospace sector is filled. Examples of applications include phones, uninterrupted power supplies, safety / alarm devices, vehicle alarms, toll collection, and asset monitoring systems, medical equipment and oil extraction.

Disposable batteries power daily objects such as remote control, torchlight, etc. Rechargeable batteries, such as alkaline batteries, are found in compact cameras, portable video game consoles, cellphones and more. Advanced batteries such as lithium batteries consume too much electricity, e.g. notebooks and other computers **[7].**

Figure 1.1 Applications of battery **[8]**

Artificial organs, hearing aids, insulin pumps, valve aid machines use batteries. Mercury batteries can be useful for optical light meters and electronic equipment, such as an alarm clock in real time. The ECG heart monitor is attached to the battery so that it can be transferred with the patient and is still on to display the patient's vitals **[7].** Rechargeable batteries, such as lithium-ion batteries and nickel-cadmium batteries, are found in hospitals.

A battery electric vehicle (BEV) that uses only the chemical energy contained in rechargeable battery packs without a secondary source of propulsion (e.g. hydrogen fuel cell, internal combustion engine, etc.). The BEVs use electric motors and motor controls for propulsion instead of internal combustion engines (ICEs). They draw all the power from the battery pack and therefore have no internal combustion engine, fuel cell, or fuel tank. BEVs include, but are not limited to bikes, bicycles, scooters, skateboards, railcars, watercraft, forklifts, buses, trucks and cars.

Batteries are found in radios that are really critical for emergency response. In order to carry huge loads, these radios require large batteries. ECGs, flashlights, and sometimes metal detectors or fire alarms require batteries **[7].** These machines help to save lives every day. Also, the batteries are operated by the radios that are used to communicate. Even the night vision, the infrared lenses are powered by batteries. Lithium has a much longer lifetime for electronics, and silver oxide batteries are used in industrial and submarine applications **[7].**

Batteries can help these consumers control their electricity by saving energy during low-cost periods and by discharging energy at high-cost periods. Batteries will store and discharge electricity from solar and wind power when it is most needed. We are therefore overwhelmed by regular battery applications, and thus batteries have become part and parcel of our lives, as new devices are based on batteries rather than traditional sources of energy.

1.4 Why lithium-ion batteries?

Batteries are important to our new technology and the choice of proper battery control is a must-have alternative. Several batteries function effectively, but lithium batteries are a better choice.

Alkaline batteries and lithium batteries are the two most commonly used battery types. These variations become more important as lithium batteries enter the AA and AAA markets that once dominated by alkaline batteries and have varying formulations of chemical compounds and voltage levels **[9].** Zinc and manganese oxide are used by alkaline batteries for power generation while lithium batteries use lithium metal or their anode compounds. Lithium batteries contain twice as much voltage as alkaline batteries, allowing them longer life, making their AA and AA models more powerful than their alkaline equivalents. The most important benefit over alkaline batteries is lithium batteries are rechargeable.

Lithium-ion batteries and NiCad batteries (nickel / cadmium) have distinct similarities. Both battery types can be recharged and are suitable for some applications. Although similar, Li-ion and NiCad batteries vary in chemical structure, environmental effects, application and expense. NiCad batteries contain between 6 per cent (industrial batteries) and 18 per cent (consumer batteries) of cadmium, which is a dangerous heavy metal and thus takes extra precautions during the removal of the batteries **[9].** The federal government classifies this as toxic waste. In the United States, half of the price of the battery is a charge for its proper recycling at the end of its operating life. Lithium-ion battery parts are environmentally friendly since lithium is a non-hazardous material **[9].**

The major downside of nickel-cadmium batteries is that they suffer from a "ghost effect" if they are depleted and recharged multiple times in the same state of charge. The battery "remembers" the point in its charging cycle when the recharging started and the voltage decreases abruptly at that point during subsequent use, as if the battery has been discharged.

However, the capacity of the battery is not significantly reduced. Any devices are specifically built to survive this decreased voltage long enough to allow the voltage to return to normal. However, certain systems are unable to function during this time of diminished power, and the battery tends to be "dead" earlier than expected.

Whereas, lithium-ion batteries are of low maintenance. They can be recharged until they are completely discharged without having a "memory effect" and work within a broader temperature spectrum. Compared to Ni-Cd, lithium-ion self-discharge is less than half, making it better suited for modern fuel gauge applications? The only downside is that the lithium-ion battery is brittle and needs a safety circuit to ensure safe operation. The safety circuit is installed into each box, which limits the peak voltage of each cell during loading and prevents the cell voltage from falling too low on discharge. The temperature of the cell is also monitored to prevent temperature extremes.

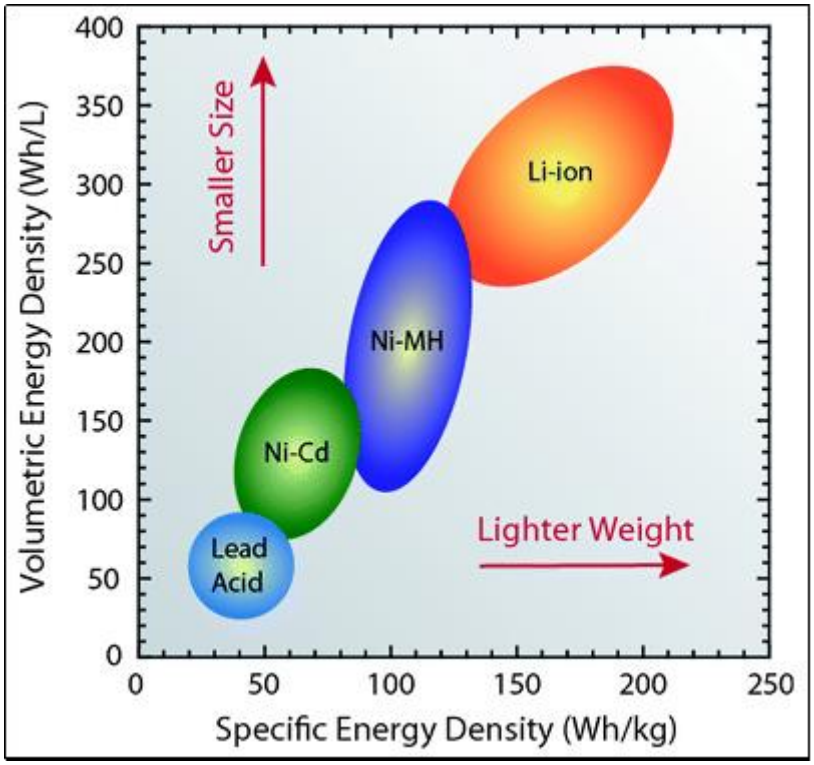

Figure 1.2: Energy densities of rechargeable battery technologies **[10]**

Li-Ion has better gravimetric density than the Ni-Cd and Ni-MH values, as can be seen from figure 1.2; which means that Li-Ion powered devices can be made much lighter without losing the running time. Also, retaining the same weight, if Li-Ion batteries are used, the runtime shall double. Because of this advantage, Li-Ion chemistry is rapidly replacing Ni-MH batteries to electrical appliances.

Thirdly, **Lead acid and lithium batteries** have a great impact in today's market. Lead acid has been going-to for more than 150 years. Most businesses fear the improvements and enhancements needed to respond to modern and changing developments. But, as the expression goes, the only thing that is steady is transition. It's time to phase out lead acid with its weight, volatile acid base and obsolete quality.

Contrary to lead acid batteries, 85 percent or more of the rated power of a bank of lithium batteries is generally used on a daily basis and often even more. Imagine the 100 amp-hour battery – if it were lead acid, you would be prudent to use just 30 to 50 amp-hours of power, but with lithium you could pump 85 amp-hours or more **[11].**

Laboratory findings suggest that you might expect to see 2000 to 5000 cycles out of a well-maintained battery bank for LiFePO4. These are theoretical findings, but recent tests show that after 2000 cycles the battery will still deliver over 75% of its power. Even the best depth batteries for lead acids are generally only good for 500-1000 cycles.

Lithium-ion batteries can be charged "fast" to 100% of the capacity. Unlike lead acid, there is no need for the absorption process to store the final 20%. And if the charger is powerful enough, lithium batteries can also be charged madly fast **[12].** If we can supply enough charging amps, we can actually fully charge a lithium ion battery for only 30 minutes. But even though we cannot get to 100%, we should not be worried, unlike lead acid, inability to charge batteries with lithium-ion is not destroying batteries on a daily basis. This gives us a lot of versatility to tap into energy sources whenever we can get them without thinking about having to do a full

charge on a regular basis. Also, lead acid batteries are less effective at generating capacity than lithium ion batteries. Lithium batteries are powered with almost 100% energy compared to the 85% efficiency of most lead acid batteries.

	Specific Energy (Wh/kg)	Specific Power (W/kg)	Cell Voltage (V)	Cycles	Life (years)	Self-Discharge Rate	Efficiency
Lead-Acid	35-50	150-400	2.1	250-1,000	5 years	20%-30%/month	75%-85%
Nickel-Cadmium	30-60	80-150	1.2	1,000-50,000	10-15 years	5%-15%/month	60%-70%
Nickel-Hydrogen	50	220	1.4	1500-6000	15 years	Very high except at low temperatures	85%
Nickel-Metal-Hydride	60-80	200-300	1.2	300-600	2-5 years	15%-25%/month	66%-92%
Lithium-Ion	80-180	200-1000	4.2	3,000	5+ years	2%-10%/month	80%-90%

Table 1.1 Comparison of key characteristics of rechargeable batteries **[13]**

Wrapping up, the thorough comparison above has led us to select lithium-ion batteries as they are safe to work with as well as unhazardous impacts on human life and also to make them an acceptable option for more high-tech work.

1.5 Literature review

For our thesis we had to consider many previous works done in order to investigate the various methods used for fast charging. Considering the sensitivity of Lithium ion batteries in terms of internal chemistry as well as the effects on its lifetime due to various differences in the charging methods, it is vital to find out the most suitable method in order to provide the best performance in terms of performance and battery life. Thus, we took the following literatures into account:

Yin et al. 2016 provides an overview of the conventional CC-CV charging system with limited fast charging. In a certain range, the pulse frequency for battery charge length is dynamically changed to inject maximum charge current into the battery cells **[14].** Indeed, in a comparatively short period of about 70 minutes a fast-charging battery charger available on the market cannot charging up to 80 percent. The pulsated charge technique was recognized as an effective and fast way to resolve the deficiency in distributed battery cells of the long charging times. The balance between the charge speed and the reliability of the internal electrochemical process, which prevents the increase of the charge rate, must be taken into account. By sensing and exchanging dynamically modified characteristics of battery status, such as voltage, injecting current, load current and operating temperature, the battery charger must monitor the reasonable current injection at an explicitly biased voltage stage. This paper describes the work to develop a fast algorithm for battery charging based on optimal frequency and duty control while also protecting battery cells against overvoltage or overheating, to provide the battery pack with a long-term cycle **[15].**

Keskin & Liu, 2015, has done more rigorous work on the PCS and DPCS method, which indicates that the pulse loading system (PCS) **[16]** is the methodology on which the proposed method is based in the paper. In this text, it has been suggested that the Dual-Pulse-Charging

System (DPCS) in both phases should be charged to increase charging time. In PCS the ions are given time to distribute uniformly during the rest cycle, but there is no rest period at a continuously loaded or multi-load algorithm. Although PCS offers a considerably longer battery life, the charging time degrades. With this process a few tens of milliseconds to lay down and stabilize ions and chemicals by using steady current for a limited period (e.g. a few seconds) The DPCS approach aims to use the rest time to increase the charging speed by using a smaller pulse.

Jiang et al. also discuss the effects of polarization and the excessive effect in 2014. The excess energy cost in the first cycle results in the excess impact. The voltage hysteresis of polarization can be observed, by contrast, while the charge current decreases a comparison between the polarization voltages under variable charging and the charge of 1/3C CC – CV, which indicates that the battery polarization tension exceeds the charge current. When charging current shifts, but due to the constant amount of time, the three processes cannot react quickly. The electrode flows through the electrode every second. The effect is caused by polarizing hysteresis. The first and second fast processes, and the third slow processes **[17].** It is obvious that the present changes lead to the hysteresis in this study and vanish as polarization of the battery becomes steady. The variable load profile is: at start up, charge the battery to 20% SOC at 1/3C and then load at 1.2% SOC at medium level with 20% – 80% SOC and at last 1/3C. The entire polarization mechanism involves at least three aspects: an electronic and ionic conduction inside the electrode, an electrical and an electrolyte interface charge transfer reaction, and the Li-ion transport process, for example gradient-driven diffusion in concentrations. The inflated amplitudes of 20% SOC and 80% SOC dots are not the same, because kinetics of reactivations are not symmetrical in the increasing and decreasing phase. The study of the characteristics of polarization voltage in the various charging levels shows that polarization voltage on both sides

is high but low on the central SOC scale. A linear relationship exists between the steady-state polarization of the voltage and the charge rate within the middle range of the SOC. Two-times voltage variance constants are 10-s and 1000-s **[17].** The magnitude orders that lead to three response charging processes. Dynamic polarization resistance shows a delayed effect and an overflow effect during operation of the battery. They are filled with various currents. This paper proposes an appropriate charging current curve, taking into account polarization time constants depending on the voltage characteristics of the polarization.

Zhang et al. **[18]** examined the impact on battery recharges and impacts of the charging system of the CC-CV on Li-ion batteries by variable temperatures and C-rate. It was noted that, irrespective of lower charging time by raising the CC phase current, this led to a longer CV phase of charging, so raising the current in the CC phase had no perceptible impact in comparison with low CC current.

Khan et al. [19] demonstrate the effects of multistage Current charge, which is a way to change current levels during the charge cycle. The findings are described in their studies. The method is followed by the reduced continuous charging current, beginning with a high initial constant current stage, in two or three stages, which finally end with the CV stage. The analysis indicates that the MSCC approach has improved the CC-CV approach by 12%.

The influence of boost charging was demonstrated in **Notten et al. [20]**'s studies. Boost charge is a procedure that first injects a high average current, followed by a very moderate current CC-CV step. In the report, a variety of different boost charging modes were tested with a boost charging time of 5 minutes on cylindrical and prismatic LCO cells. In contrast to the conventional 1C CC-CV process, it was observed that this process increased the charge speed by a substantial 30%-40%.

Jun et al. [21] demonstrates a major effect of a 1C pulse loading on the loading time. Pulses are charged in order to allow for brief rests, which does not affect the battery **[22],** when charging the battery with charging current with occasional pauses between them. The study has demonstrated that 1C pulse charge can reduce the charge time from 3.5 to 1 hour by pulse load, as the CV loading process was not present **[21].**

Thus, we can observe that many various studies provide different pathways to introduce faster charging of Lithium Ion batteries. This study considers the pulse charging method and the double pulse charging method and aims at merging the two methods to provide a more innovative way of obtaining faster charging.

1.6 Thesis objective and outline

Our objective is to design a charging system which provides a faster charging using the Double pulse methodology while maintaining an optimized frequency and duty cycle in order to obtain a faster charging as well as an optimal result to ensure faster charging and minimum damage done to the battery. Basically, this thesis consists of 5 chapters,

- **Chapter 1** presents an introductory part with motivation, applications of battery, importance of lithium-ion batteries and fast charging setup, thesis outline and objective.
- **Chapter 2** provides a comprehensive overview of battery along with difference between rechargeable and non-rechargeable batteries, battery charging and discharging mechanism, terms associated with battery as well as equivalent circuit modelling and the proposed method.
- **Chapter 3** comes with simulation which includes the charging environment, battery parameter estimation and modelling along with C-rate and frequency effects, and finally design and simulation of single pulse charging system with comments on the drawbacks.
- **Chapter 4** deals with the design of the double pulse charging system and presents the difference between the outputs of the SPCS and the DPCS. The results of varying duty cycle of secondary pulse with and without current limiter, analyzing the temperature effect and charging rates are shown in this chapter. This is followed by finding the optimal charging condition from the data obtained for the double pulse charging system, comparison and improvements over previous methods.
- **Chapter 5** summarizes our contribution in this project with possible future works.

Chapter 2: Lithium-Ion battery fundamentals

2.1 Introduction

In this Chapter, we introduce the properties and operation of lithium ion cells which is the vital element of our thesis work. This includes the internal properties of the battery and the different types of available Li-ion Batteries. The mechanisms of charging and discharging batteries are also discussed as this is the main purpose of this thesis. Important terms related to batteries and charging have been mentioned as they are used throughout the paper followed by the equivalent circuit model of the Li-ion battery. This circuit model is crucial for explaining the use of the methodology of variable frequency and duty cycles which is explained towards the end of the chapter. The methodology also includes the key concepts of design and implementation of the existing and proposed charging methods.

2.2 The battery

A battery is an apparatus that converts chemical energy into electricity upon release. This is achieved by means of two important chemical reactions, oxidation and reduction. There are two major types of batteries: primary and secondary. Primary batteries are ones that cannot be recharged because the chemical reaction inside the battery cannot be reversed and needs to be discarded until finished. Secondary batteries can be recharged and re-used many times. A Li-ion battery usually refers to a secondary battery.

2.2.1Operation of lithium-ion cells

In a lithium-ion battery cell, both electrodes depend on the mechanism of the intercalation rather than the standard red-ox chemical reaction. Intercalation is a method of reversibly withdrawing or introducing metal ions into a host without a major structural change to the host

[23]. Lithium-ion cells are able to store lithium in either one or both of the electrodes. The lithium that reaches the electrodes is contained in the electrodes just as water is retained in a sponge; the composition of the electrodes does not change itself.

A lithium-ion battery essentially has five primary components:

- Positive electrode
- Negative electrode
- Separator
- Electrolyte
- Current collectors

2.2.2 Positive electrode

The first intercalation material that was discovered for positive electrodes and lithium-ion battery cells was lithium cobalt oxide (LiCoO2) or LCO. Professor Goodenough and his research team discovered that material in 1980. In fact, lithium cobalt oxide makes quite a good material for positive electrodes, and it is in very common use **[23].** In a lot of handheld electronics and tablets and smart phones, but as we want to scale up the lithium cobalt oxide to very large battery cells and very large applications, there are certain difficulties. Think of vehicle use or utility grid use, for example. One of the issues is that cobalt is very rare, and so it's costly. It's also a toxic element and so we don't want to have too much of it thrown out by accident and landfill entry **[23].** Another obstacle that might not be immediately evident with lithium cobalt oxide is that we can only use about half the potential ability. So, to make this material more practical for large scale application, researchers have replaced some of the cobalt in the structure with different elements. If we replace all the cobalt with nickel, then we end up with lithium nickel oxide. And for the same amount of material, that has actually a higher energy density, so we can store more energy **[23].** Currently, the most popular substitution is

replacing some of the cobalt with nickel and some with manganese. And so, we end up with a material called nickel cobalt manganese or NCM. Many car battery packs are made of this type of NCM or NMC battery cell. Another option is to substitute some of the nickel cobalt and others with aluminum, and this is an NCA battery cell. And this is the type of battery cell that is being used at this point in time in Tesla automobiles **[23].** A major advantage of lithium manganese oxide over lithium cobalt oxide, or even NMC or NCA, is that it's less costly because manganese is so natural, and therefore cheaper. The oxide is less reactive than the phosphate. It also has a high density for power. A major weakness of LFP is its low electrical and ionic conductivity.

2.2.3 Negative electrode

Essentially all commercial lithium-ion battery cells use some form of graphite at this point in history for their negative electrodes. Graphite is one form of carbon and is formed by stacked together layers of grapheme **[23].** The voltage of a battery arises from the difference in reduction potential between the graphite anode and the cathode material. LCO has the highest range of operating voltages, followed by NMC and NCA. The lowest range is for LFP. LTO is known for its high-power density and cycle life **[23].** Compared with graphite, it has a greater surface area which allows more lithium ions to be injected into the material. And many of the reactions that degrade graphite do not occur with LTO during cycling. LTO's use is limited by its low voltages and energy density.

2.2.4 Electrolyte

Electrolyte is the medium that transports ions inside the cell between the electrodes. And that the electrolyte in a general electrochemical cell consists of a solvent in which we dissolve either a salt, or an acid, or a base. Some battery cells use an electrolyte whose solvent is water and we

call those aqueous cells. But any battery cell with a voltage greater than 2 volts is not allowed to use water as its solvent. A lithium ion battery cell has voltages usually higher than 3V. The lithium-ion battery cells are made from non-aqueous electrolytes and are made from organic solvents plus a lithium-based salt that dissolves into that solvent. The electrolyte works simply as an ion conductor in a lithium-ion battery cell **[23].** This does not take part any in the usual chemical reactions for battery cell charging and discharging. The most common solvents in the lithium-ion battery cells used in electrolytes that are ethylene carbonate, propylene carbonate, dimethyl carbonate, ethyl methyl carbonate, and diethyl carbonate **[23].**

2.2.5 Separator

Lithium-ion battery cells require a separator too. The separator is a permeable membrane that contains tiny holes and these holes are sufficiently wide to allow ions to travel into them, but they are still small enough that the positive and negative electrode cannot reach one another. If they touched each other there is a chance to have a short circuit, leading to heat buildup and thermal runaway, possibly a fire or an explosion. That's why the separator show in figure 2.1 must also be an electronic insulator. We can't allow electrons to flow across the separator but we want ions to flow through the porous in the separator very easily.

2.2.6 Current collectors

The lithium-ion battery cells also have current collectors. And these are made of metal foils that deposit the electrode materials onto. The current collector’s purpose is to conduct electrons from the materials of the electrode to the tabs of the cell terminals to the outer circuit. And these foils are subjected to very harsh environments inside the cells.

In every positive electrode current collector are made with aluminum foil. It is chosen because aluminum tends not to react to anything as long as its potential is about 3 volts or higher. And

all of the positive active electrode products are selected to have higher potentials. So instead, they do not interfere with this aluminum and do any harm to it in the usual working area of the lithium-ion battery cell. In the negative electrode, the current collector's almost always a copper foil. And that's, again selected because the copper is electrochemically stable and does not react with any potential lower than around 2 volts.

2.2.7Cell format

LIBS are available in three formats, such as:

- Cylindrical Cell
- Pouch Cell
- Prismatic cell

Within a cylindrical cell (Figure 2.1a), alternating layers of the electrode materials are packed in a jelly-roll structure and mounted in a metal tubular case. The electrode materials are placed in alternating layers in a pouch cell; the stack is then filled with a metallic plastic and sealed to form a so-called pouch (Figure 2.1b), The electrode materials can be wrapped or stacked in a prismatic cell and are mounted in a rectangular metal case **[23].** In everything from laptops to Tesla vehicles are found cylindrical cells. Pouch cells come in all sizes and are used in drones and other vehicles with cell phones. Prismatic cells (Figure 2.1c), are usually used in the automotive industry.

The most common type for LIBs is cell has strong mechanical stability; rolling the jelly enables more material to be packed in the cell, resulting in high energy Scale. And distance the cell has strong mechanical stability; the tubular casing without deformation can withstand high internal pressure **[23].** However, the performance of cylindrical cells for packaging is poor. The prismatic cell with a higher packing performance will achieve a comparable energy density.

Prismatic cells are, however, more costly to manufacture than cylindrical cells. The pouch cell is the lightest and smallest format, and has the best efficiency in packaging. It also needs support, because the cell is soft and expanding. In this thesis, we will be using the cylindrical cell for our simulation cylindrical cell.

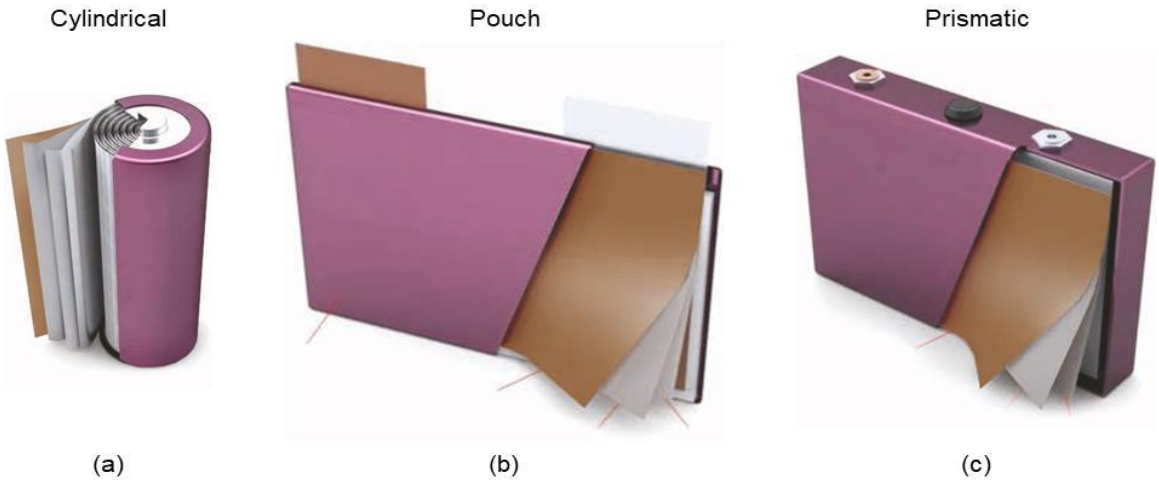

Figure 2.1: Formation of different types of Li-ion battery cells: a) Cylindrical Cell b) Pouch Cell c) Prismatic Cell **[24]**

2.2.8 Charging and discharging mechanism:

The lithium-ion battery consists basically of two electrodes, electrolytes and separator as shown in Figure.1. A lithium containing transition metal oxide such as LiCoO2, LiNiO2, and LiMn2O4 in positive electrode is used to supply the active substance lithium ion. The lithium ion working substance found in is coke, graphite, amorphous carbon in negative electrode, and so forth. Electrolyte is dissolved in organic solvent lithium chloride, lithium salts are LiPF6, LiAsF6, LiClO4 etc. and organic solvents are ethylene carbonate, propylene carbonate, dimethyl carbonate, and chloro carbonate. Lithium-ion batteries conform to the concept of "rocking chair" when charging and discharging **[25].** The exchange of ions and electrons takes

place in lithium ion battery during electrochemical reaction which is a redox process. During the charging process Li^+ anode ions (positive electrode) pass into the cathode (negative electrode). Hence, the positive electrode loses electrons (oxidation) and the negative electrode absorbs electrons (reduction) during the charge process. The reversed things happened during discharge process. The electrochemical reactions are shown from equations 1-4.

Positive reaction:

$$Li_{1-x}MO_2 + xLi^+ + xe^- \xrightarrow{\text{Discharging}} LiMO_2 \quad (1)$$

$$LiMO_2 \xrightarrow{\text{Charging}} Li_{1-x}MO_2 + xLi^+ + xe^- \quad (2)$$

Negative reaction:

$$Li_xC_6 \xrightarrow{\text{Discharging}} xLi^+ + xe^- + C_6 \quad (3)$$

$$Li^+ + xe^- + C_6 \xrightarrow{\text{charging}} xLi_xC_6 \quad (4)$$

2.3 Terms associated with standby batteries

There is also a term used in the field of batteries and chargers that may contribute to some confusion. This section clarifies this complexity by a brief section describing each term. The terms are used throughout this thesis.

2.3.1 Cell nominal voltage

A nominal voltage, a normal voltage or even an average voltage of a battery cell, anywhere between a cell's fully charged voltage and a cell's fully discharged voltage. For many nickel-

based cells it is around 1.2 v and for lithium ion cells it is around 3V. It is often printed on the cell package.

2.3.2 Cell capacity

It specifies the quantity of charge that the cell is rated to hold. The unit of it is Ampere hour (Ah) or mill ampere hour (mAh). If a battery cell has a capacity of one Ampere hour (Ah), then a fully charged cell can deliver one Ampere of current for the period of one hour before it is fully discharged. At the beginning of life, most battery cells will actually have slightly higher capacity than what is printed on the package. And over life, for various reasons the capacity will decrease.

2.3.3 C rate

A relative measure of electrical current that is somehow scaled to the size of a battery cell, and this relative measure is known as the C rate **[26].** The C rate of a battery cell is the level of constant current charge or discharge that the cell can sustain for one hour of time. For example, a cell having a capacity of 20 ampere hours should be able to deliver 20 amperes of current for one hour or two amperes of current for 10 hours. When the cell should be able to deliver 20 amperes of current for one hour then it can be said that the C rate of a 20-ampere hour cell is 20 amperes. It’s called 1C rate.

2.3.4 Energy and power

A cell stores energy in electrochemical form, which it can later release to do work. The total energy storage capacity of a cell is roughly its nominal voltage multiplied by its nominal capacity (mWh, Wh, or kWh) **[26].** Considering the cell nominal energy storage capacity is

3.7V multiplied by 1.9Ah, which gives us 7.03Wh.Energy and power are different things. The energy release rate is the cell's instantaneous power (mW, W, or kW).

2.3.5 State of charge (SOC)

State of Charge applies to the proportion of the overall energy power of a battery which is still usable for discharge. This is loosely comparable with the fuel tank of a vehicle, where 0 percent is empty and 100 percent loaded.

2.3.6 Depth of discharge

The amount of energy drawn from a battery (or battery pack), usually expressed as a percentage of the battery's overall power. For example, 50% discharge depth means half the energy was used in the battery **[26].** 80% DOD means eighty percent of the energy was discharged and the battery only retains 20 percent of its maximum capacity.

2.3.7 Cycle life

For rechargeable batteries, the total number of charge/discharges cycles the cell can sustain before its capacity is significantly reduced. End of life is usually considered to be reached when the cell or battery delivers only 80% of rated ampere-hour capacity **[26].** A battery cycle is highly affected by cycle type depth and recharging process. Improper cut-off in the charging cycle will significantly reduce a battery's cycle life.

2.3.8 Over and under potential

The voltage measured at the terminals when charging or discharging a battery, especially at high currents, does not reflect the actual Electro Magnetic Force (EMF) that the battery will supply at its current SOC **[26].** The calculated voltage should be lower when discharging occurs

than the real EMF. The difference is considered the Battery's under potential. The calculated voltage would be higher during charging than the actual EMF which generates an over potential.

2.4 Equivalent battery model

Batteries resistive and capacitive properties arising primarily from polarization phenomena and cell ohmic resistance. For the resistor R1 and the capacitor C1, the capacitive impedance generated by polarization phenomena can be simulated which is shown in on (Figure 2.3)

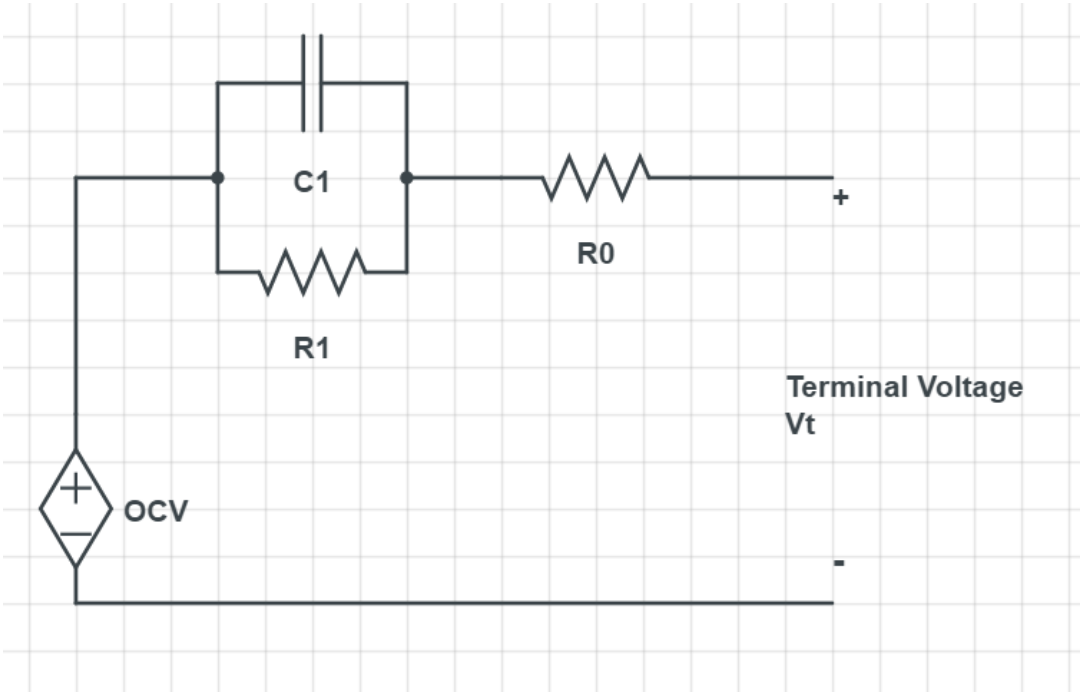

Figure 2.2: Equivalent Battery Model (Modelled in circuitlab.com).

Where Ro is the battery's internal ohmic resistance, R1 and C1 are the resistance to polarization and the capacitance to polarize, all of which form the RC circuit to define the batteries polarization. Here also OCV (z(t)) is open circuit voltage which is controllable and generally varies non-linearly with SOC. Finally, V(t) reflects the voltage of the battery terminal, determined directly by the voltage sensor.

2.5 Methodology

The charging rate in a battery is an important parameter for determining the charging speed which is permitted in terms of reliability. The SOC refers to how much charge is present in a battery. The SOC is proportional to the available charge as compared to the fully charged battery state. A high polarization voltage is observed at an SOC lower than 20 percent and higher than 80 percent, while it is relatively small when SOC is over 20 percent and under 80 percent as presented in figure 2.3. **[14]**

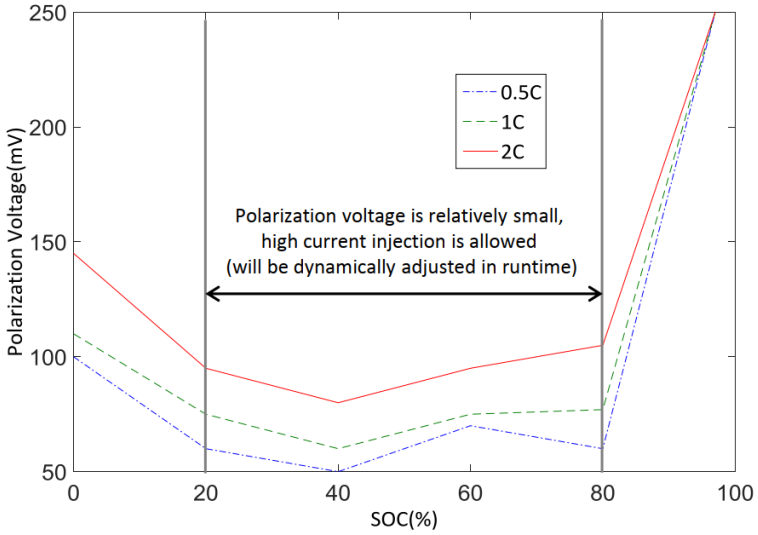

Figure 2.3: Polarization Voltage over various SOC **[14]**

The allowed current injection is limited by considering the battery's SOC, based on the polarization mechanism. Therefore, a suitable appropriate charge current requires to be obtained the charge period either by raising the charge rate to reduce the time or by reducing the charge rate to limit the damage to the battery. As it is observed in **[17]** high current rates lead to high polarization, thus the use of lower current at low SOC is essential. Considering the polarization at higher SOC we can use higher current while reducing the average current injected by every 5% of SOC to prevent overheating and further damage to the battery due to high polarization, and as soon as SOC reaches 80% charging will be stopped. The acceptable

charging current based on polarization chart for the INR18650-25R 2.5Ah battery is given in table 1 **[[14], [17]]**

SOC Range (%)	Charging Current (A)
0-20	1.25
20-40	4
45-50	3.858
50-55	3.539
55-60	2.979
60-65	2.659
65-70	2.319
70-75	1.959
75-80	1.5

Table 2.1: Acceptable Charging current of INR18650-25R **[14]**

During the charging process, we simultaneously change the duty and frequency of the charging pulse to determine the appropriate injection current. The battery cell's capacitance characteristic creates different responses at different frequency pulses which are triggered while charging the battery. This is due to the RC branch in the equivalent circuit model as discussed in section 2.2

$$Z_1 = \frac{R_1 \frac{1}{jwc_1}}{R_{1+} \frac{1}{jwc_1}} \tag{5}$$

$$Z = Z_0 + Z_1 = R_0 + \frac{R_1 \frac{1}{jwc_1}}{R_{1+} \frac{1}{jwc_1}} \tag{6}$$

From equations 5 and 6 we can observe that impedance Z_1 is more dependent on the pulse charging frequency then the effects of changing SOC on the capacitive values. We can observe an inverse relation between the impedance and the frequency thus Z_1 will drop when frequency rises. The frequency range used in this thesis is from 1 Hz to 11 Hz by rising the frequency by steps of 1Hz. Such small values of frequency were used compared to the original large values of 500Hz in **[14]** due to the limitations in performance of MATLAB/Simulink in our simulation. In the process the circuit model component values were scaled to match experimental data.

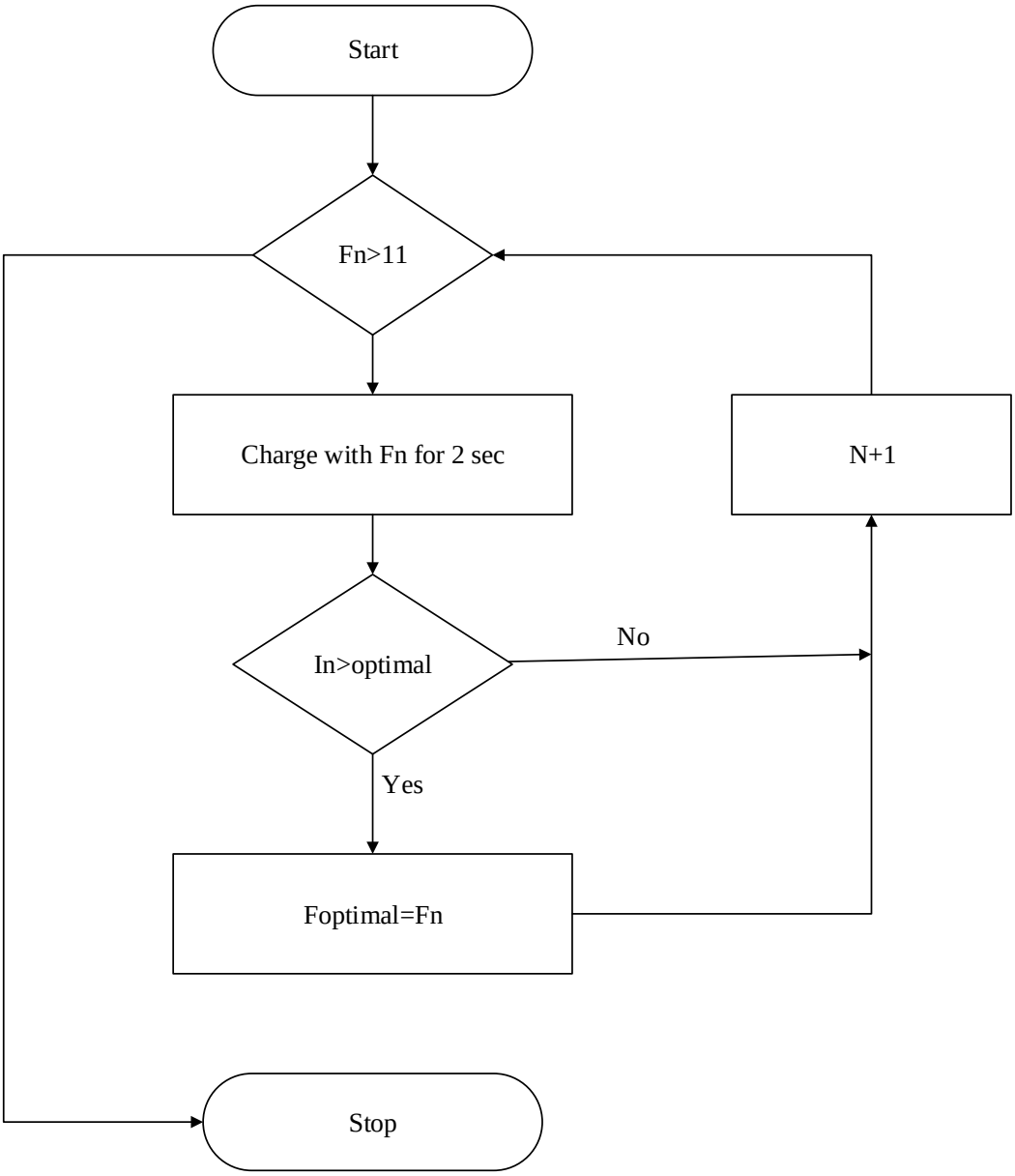

Figure 2.4:Flowchart for Frequency searching Algorithm

The algorithm for the frequency searching method shown above in figure 2.4 is explained. Firstly, the pulse frequency is configured as 1 Hz, the duty cycle is set at 50%, the optimum current (Ioptimal) is initialized as 0A and the optimal frequency ($F_{optimal}$) is initialized as 1 Hz as expressed in equations 7 and 8:

$$F_N = N * 1Hz(where\ , N: 1 \ldots .11) \quad (7)$$

$$I_N = 0A(where\ , N: 1 \ldots .11) \quad (8)$$

Then the battery will be charged for 2 seconds by F_N, the total charging current in the last two seconds is obtained followed by an update of the correspondingI_N. If (I_N >$\mathrm{I_{optimal}}$), both the $\mathrm{I_{optimal}}$ and the related $\mathrm{F_{optimal}}$ will be modified with newer I_N andF_N. F_N Can rise by steps of 1 Hz until the frequency reaches 11 Hz or when the SOC reaches 0.8. Here we can achieve the optimum frequency at which the impedance of the battery is extremely reduced and the greatest charge current is pumped into the battery cell.

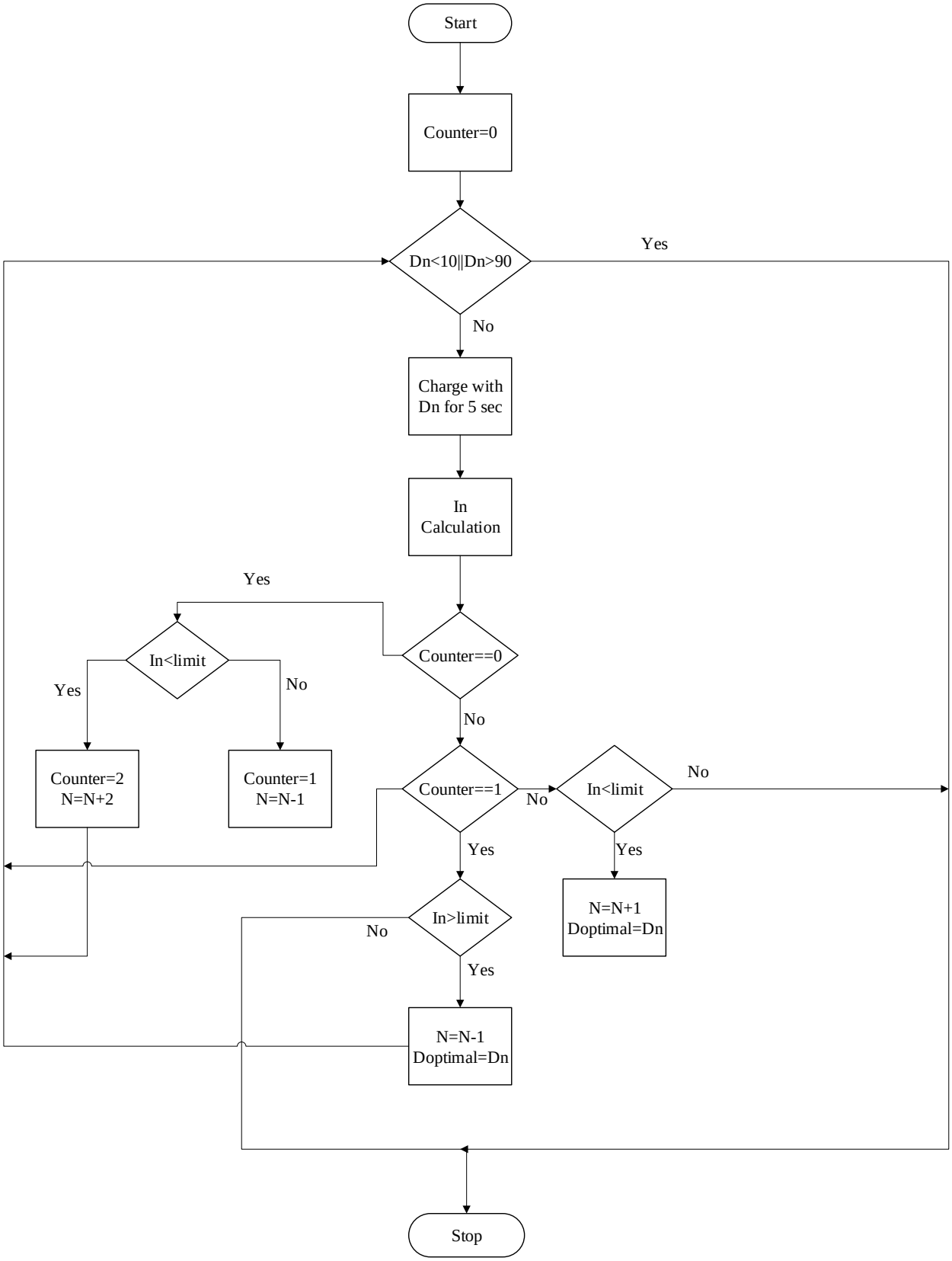

Figure 2.5: Flowchart for Duty searching Algorithm

Next comes the duty cycle search algorithm as shown in figure 2.5. Once the frequency searching is complete. The duty cycle search mode focuses on finding a reasonable length for the relaxing duration, which may be a value that is neither too short in diffusion nor too long in extending the charging time.

The optimum frequency obtained from the previous mode, at the beginning will be initialized. The 10% duty cycle will be taken as initial value and it will help to charge for next 5s. The equation 9 shows the duty cycle at for each step n.

$$D_n = n * 0.05(where\ , n: 2 \dots 18) \tag{9}$$

I_N is the equivalent charge current and I_{limit} is the appropriate corresponding acceptable current based on SOC which in turn is based on the polarization curve. To find I_N we use the equation 10 and 11:

$$T = T_c + T_r = \frac{1}{F_{optimal}} \tag{10}$$

$$\mathrm{I_N} = \frac{\mathrm{I_T} * \mathrm{T_c}}{\mathrm{T_c} + \mathrm{T_r}} \tag{11}$$

Where Tc is the charging period, Tr is the relaxation period, $\mathrm{I_T}$ is the charging current during the charging period, and I_N is the Average charging rate for a period of 1 second. After obtaining the average current, the value is compared with I_{limit} to determine whether the duty cycle should be raised or lowered in order to match the limit. In the event that the average current is lower than the limit during the first check while counter=0, counter will be set to 2 and duty cycle will be raised by 5% in the following checks and $D_{optimal}$ will be adjusted as newer D_n when $I_N > I_{limit}$, but in case the duty cycle reaches 90% or SOC reaches 0.8 the sequence will be terminated. Similarly, if the average current is higher than the limit at first check while counter=0, the value of counter will be changed to 1 and the duty cycle will be lowered by 5% in the subsequent checks until the $I_N < I_{limit}$, where the $D_{optimal}$ will be

configured as the newer D_n. Also, if the duty cycle hits 10 percent or SOC reaches 0.8, the entire duty searching sequence will be terminated.

As shown in figure 2.6 .The final step in this method is to constantly monitor the battery status and repeat the search algorithms to obtain the most optimum frequency and duty cycle in order to charge at a fast rate while simultaneously keeping the cell polarization at a minimum. To do so, monitoring of whether the SOC is divisible by 5 or not, the optimum frequency or the optimal duty cycle is sought respectively. These optimal values of frequency and duty cycle must be obtained repeatedly by repeating the proposed search mode as the conditions of the battery state vary significantly.

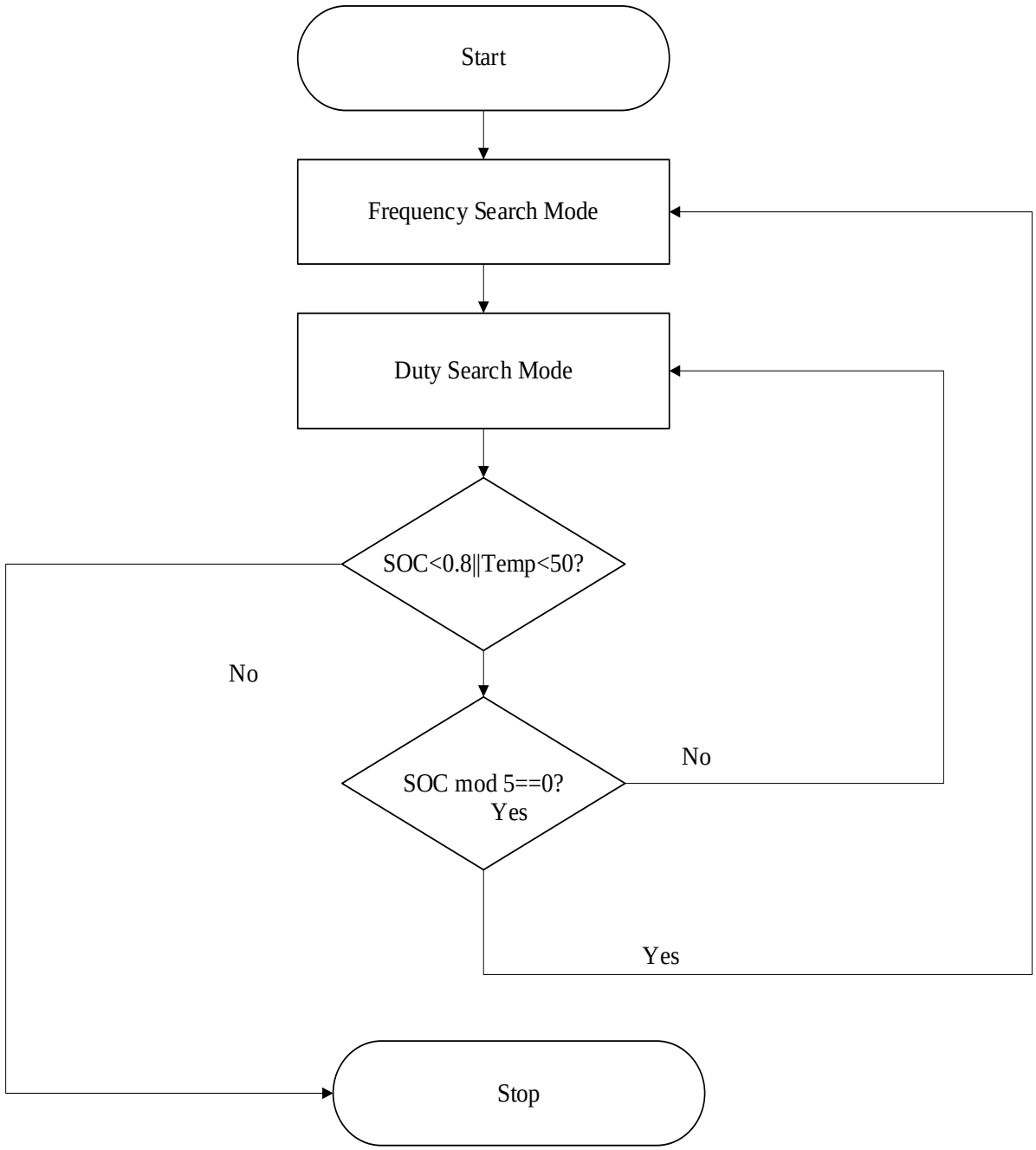

Figure 2.6: Flowchart for frequency and duty control searching Algorithm

Once the PCS charging method was simulated in Simulink, our next objective was to implement a DPCS. In this method, two non-overlapping pulse had been used. During charging time, a primary phase will help the battery to be charged up with maximum current while the

secondary phase of the battery is left to rest. If we connect the battery with another current source during the resting period of the primary phase, the secondary phase can then charge up the battery with a small amplitude current. Besides this, the battery charging system can vary the pulse width. Hence, a faster charging method can be achieved.

To sum up, we combined the two methods together to obtain the fastest charging time possible. First, the SPC method with a Variable Frequency and Duty Cycle Charging system is created and combined with the DPCS. In our design of the DPCS, we created a model where we could vary the periodicity automatically and vary the ON time of the secondary pulse.

2.6 Conclusion

We have observed in this chapter regarding battery characteristics and the various terms related to it. Furthermore, the equivalent circuit of the Li-ion battery proved how the charging methods are designed to provide the maximum possible current to the battery while considering the polarization and temperature rise of the battery. Each of the methods stated in the methodology was implemented in MATLAB/SIMULINK to prove the existing single pulse charging method discussed in chapter 3 followed by the proposed method involving the double pulse charging system with and without the implementation of using a current limiting technique in chapter 4.

Chapter 3: Single Pulse Charging System (SPCS)

3.1 Introduction

In this chapter, we discuss the implementation and results of the single pulse charging system followed by the drawbacks of this system. The single pulse system has previously proved to be a better solution over the traditional methods available. This chapters aims at recreating the battery model and charging environment using Simscape for physical modelling and state flow diagrams to design and implement the charging system.

3.2 Designing of SPCS

3.2.1 The charging environment

The following figure 3.1 shows the environment built in MATLAB/SIMULINK for the charging system of the Single Pulse Charging System (SPCS):

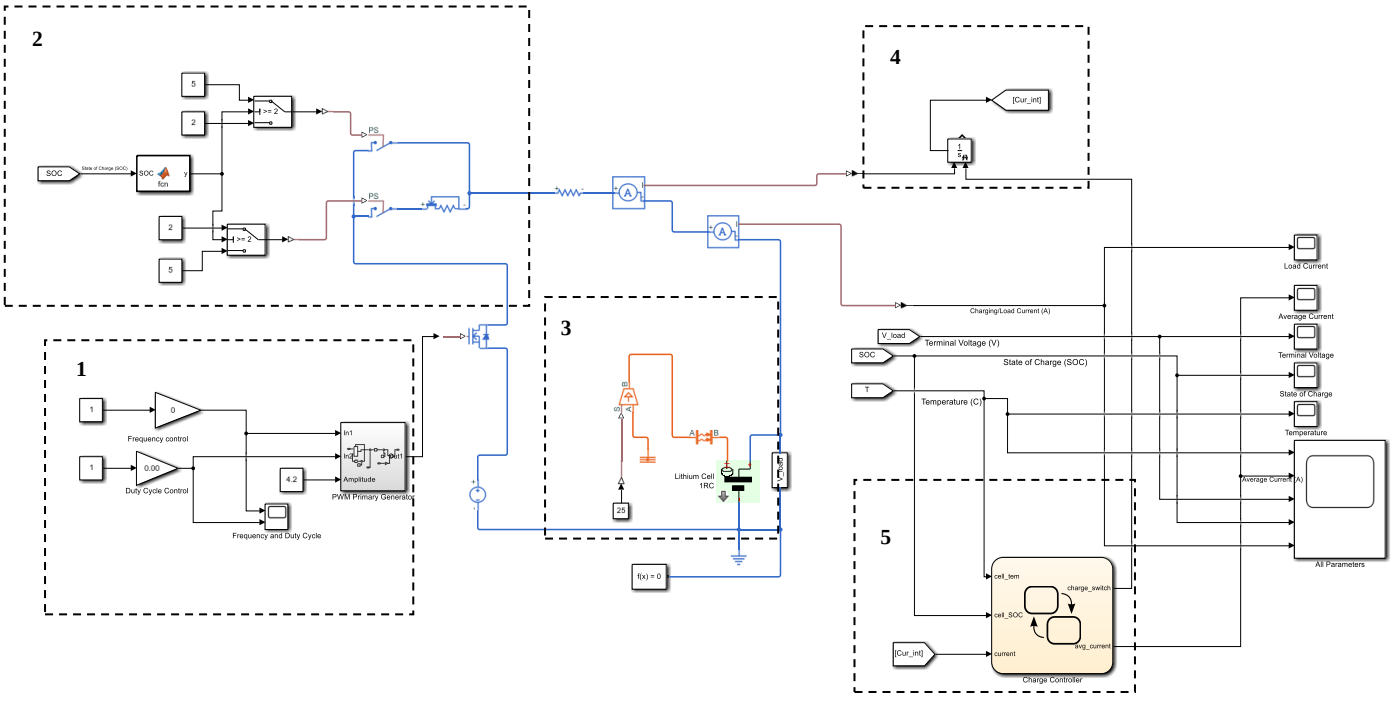

Figure 3.1: Charging environment in Simulink

Each component is labelled and explained as follows:

1. **<u>Pulse Width Modulation (PWM) primary generator:</u>** The PWM generator is one of the most crucial parts in the whole system. It functions to create a pulse of signals with different Duty cycle and Frequency manipulated by the charge controller. The 'Frequency control' gain block and the 'Duty Cycle' gain block are changed during the simulation runtime, and varied to obtain the optimal values for charging the battery. The PWM generator block built in Simulink is shown in figure 3.2.

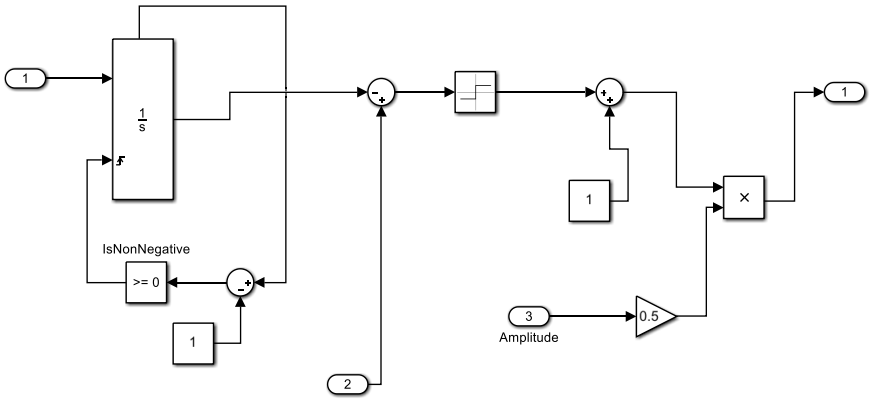

Figure 3.2: PWM Generator Block

Where ports 1,2 and 3 represent the Frequency, Duty cycle and Amplitude respectively. The output port provides the output pulse to the MOSFET as shown in Figure 3.1 to control the amount of current injected to the battery.

2. **<u>Upper/Lower channels</u>:** The channels in the system are used to direct the current through the lower channel when the SOC is below 20 percent and through the upper channel once the SOC is greater than 20 percent. As discussed earlier in section 2.5 the current injected into the battery during the first 20 percent must be small due to high polarization. Therefore, applying 4.2V directly without a current limiter would lead to a very high initial current which would

immediately result in battery damage and higher temperature rise due to the polarization. Hence, a current limiter of 1.525A is placed through the lower channel. The switches in the channels are controlled by the MATLAB function which sends the required signal to the switches based on the SOC that is inputted to the function block.

3. **Battery:** The 1RC li-Ion battery model provided by Simulink **[27]** was used in this simulation to simulate the charging scenario of the INR18650-25R 2.5Ah battery. The model has three terminals, the positive, negative and H terminal. The positive and negative terminals are connected to the charger and ground respectively. The H terminal is used to portray the heat effect on the battery due to charging. A controlled heat source is used to provide the ambient temperature, which in this case is 25 degrees. A thermal reference is also connected to the heat source which in turn connects to a convective heat transfer block to produce the exchange of generated heat in the battery with the surroundings. The thermal properties of the batteries such as the specific heat, dimensions, convective heat transfer coefficient constant etc. are specified in a workspace**. [27]**
4. **Integrator for charge accumulation:** An integrator block is used to accumulate the charging current obtained from ammeter1 for a specific period of time, in this case for 5 seconds and is fed to the charge controller for average current calculation. It is reset by the charge controller, when according to the requirement mentioned in the charging algorithm, by controlling the charge_switch from the controller.
5. **Charge controller:** The charge controller is the heart of the whole system. It obtains information about the battery SOC, temperature, terminal voltage and charging current in order to implement the algorithms and find the optimal charging current by varying the duty cycle and frequency while at the same time monitoring the temperature and the SOC to check that these parameters are within acceptable limits. The working of the charge controller will be explained in more detail later on in this paper.

Apart from the components mentioned, the system in Simulink requires a solver configuration to run the Electrical Simscape Model. An electrical reference and a thermal reference for the thermal modelling is necessary. Scopes are used to observe each parameter separately, and one large scope to check all parameters together.

3.2.2 The charge controller

Figure 3.3 on the next page shows the state flow design created using Simulink state flow inside the charge controller to implement the variable Duty and frequency searching method in order to charge the battery using single pulse technique.

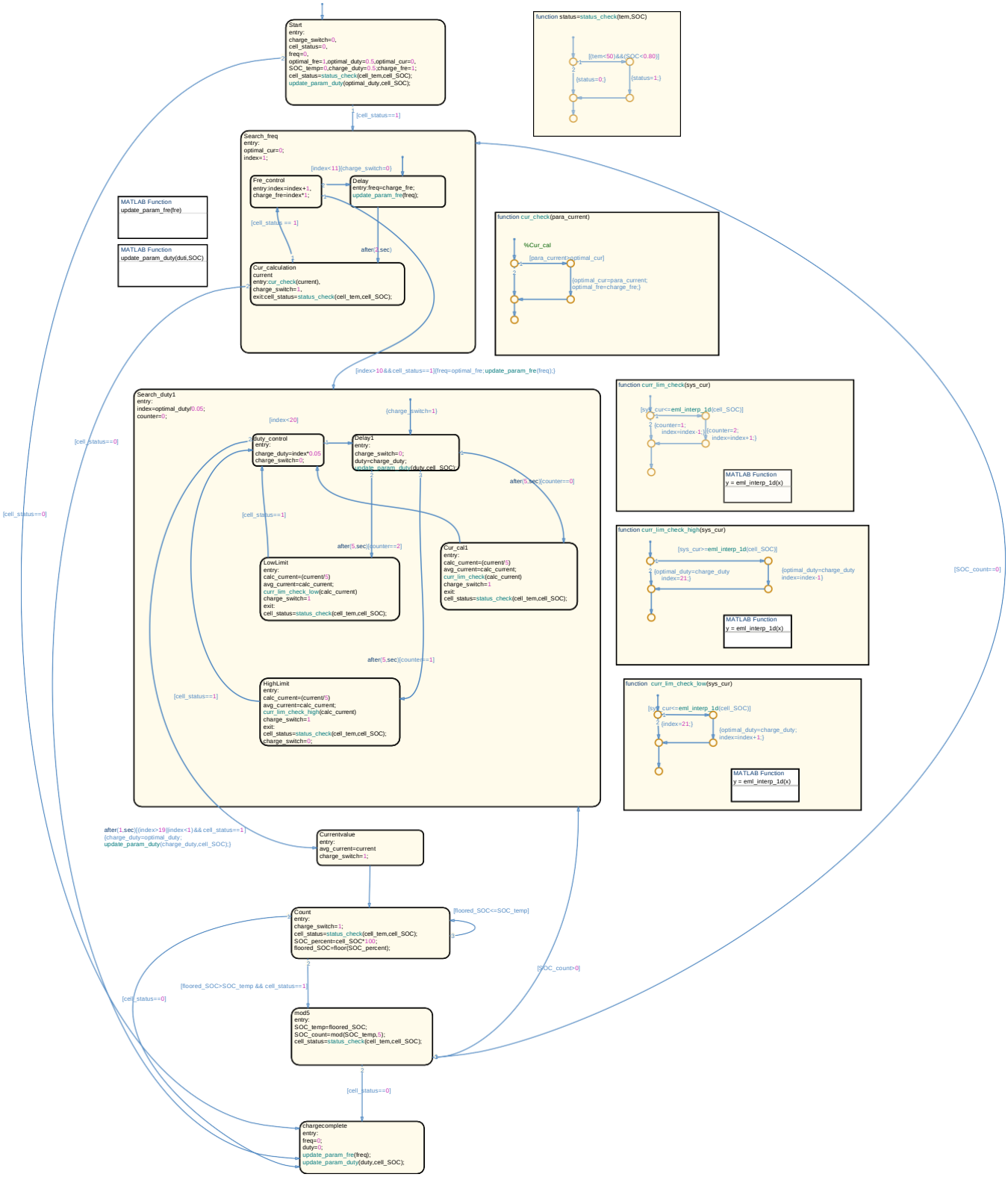

Figure 3.3: State Flow diagram inside Charge controller

Each mode is discussed as follows:

Start mode: The state flow starts with a 'Start' mode where each variable to be used within the controller is defined with an initial value. The function 'Cell status=status_check (cell_tem, cell_SOC)', which can be seen at the top right, is used to check at regular intervals at each step in the controller to determine that the battery is within 80 percent SOC and lower than 50 degrees, otherwise it would directly terminate the charging sequence by making cell status=0 and moving to the 'Chargecomplete' block at the bottom of the state flow.

Update_param_fre and Update_param_duty functions: These are important functions that are required to obtain and change the values of the Frequency and Duty gain blocks during the runtime of the simulation to allow to find the optimal frequency and duty cycle. The functions are shown as follows:

For Update_param_fre Function:

```
function update_param_fre(fre)
coder.extrinsic('get_param')
coder.extrinsic('set_param')

paramvalue = char(get_param('battery_model_final_SOC/Gain1','Gain'))
str2double(paramvalue);
set_param('battery_model_final_SOC/Gain1','Gain', int2str(fre))

end
```

For Update_param_duty function:

```
function update_param_duty(duti,SOC)
coder.extrinsic('get_param')
coder.extrinsic('set_param')
socvalue=SOC;
getvalue = char(get_param('battery_model_final_SOC/Gain2','Gain'))
setvalue=sprintf('%.2f',duti)
set_param('battery_model_final_SOC/Gain2','Gain', sprintf('%.2f',duti))

end
```

Search_freq mode: The ‘Search_freq’ mode is used to search for the optimal frequency by changing the frequency of the input from 1Hz to 11Hz and setting the frequency at which the charging current to the battery is the highest as the optimal frequency. The function ‘Update_param_fre’ is responsible for changing the frequency gain block of the PWM generator during the simulation. As before, the cell status is monitored before moving onto the next searching mechanism to ensure the battery is within the restrictions mentioned previously.

Search_duty1 mode: The ‘Search_duty1’ mode is used to vary and obtain the optimal duty cycle to match the average current input to the battery. The accumulated current input to the battery is obtained through the integrator block via the ‘Cur_int’ from and goto blocks. The Charge_switch controls the reset button of the integrator to reset the accumulation of current to be averaged after every 5 seconds. The calculation is done first in the ‘Cur_cal1’ state, while counter is set to 0, where it determines whether the duty cycle should be incremented or decremented by comparing to a set LUT table based on the acceptable charging current of the battery for any particular SOC. To do this, the accumulated current from the integrator is averaged. The averaged current is then sent to the function ‘cur_lim_check(sys_cur)’ and compared with the table. If the averaged current is higher than the limit, the counter is set to 1 and the state moves to the ‘HighLimit’ state where it slowly decreases the duty cycle until it is below the limit defined by the LUT or reaches minimum 10 percent. On the contrary, if the average current is lower than the limit, the counter is set to 2, moving onto the ‘Low Limit’ state, raising the duty cycle by 10 percent just until the limit is exceeded or reaches a maximum of 90 percent duty, thus maintaining fast charging without damaging the battery. Once the correct value of duty cycle is obtained, it is stored in the optimal duty and set into the Duty gain block via the ‘Update_param_duty’ and exits the state.

CurrentValue mode: The ‘CurrentValue’ state is used to measure the new average current after finding the optimal duty cycle and is sent to scope via the avg_current line.

Count mode and mod5 mode: The state flow then moves onto the ‘count’ state where the SOC is calculated in percentage and floored which is required for the next state, ‘mod5’. This state checks the value of SOC by calculating the mod of the SOC by 5 at every 5 percent of the SOC to search for the optimal frequency once again. This is important as the battery characteristics change rapidly and thus the frequency and duty cycle require to be checked at regular intervals. If the battery is at a 5 percent interval, SOC_count will be set to 0 and the optimal frequency will be searched followed by the duty search, otherwise the SOC_count will be set to a value greater than 0 and the search will return to duty cycle search only.

It is vital to note that at every state, the battery status is monitored to maintain the limits of the battery. Once the battery reaches 80 percent of SOC or reaches a temperature of 50 degrees, the charging will be stopped immediately to prevent damage to the battery.

3.3 Estimating battery parameters

To create an accurate model of the INR18650-25R the LUT values for Em, R0, R1 and C1, which stand for the open circuit voltage, internal resistance, capacitive resistance and capacitance respectively, as observed in figure 3.4 for the 1RC model of the battery equivalent model were varied through trial and error. The values in each table are changed and the simulation is run continuously to try and converge the simulation result with experimental data in **[13]**.

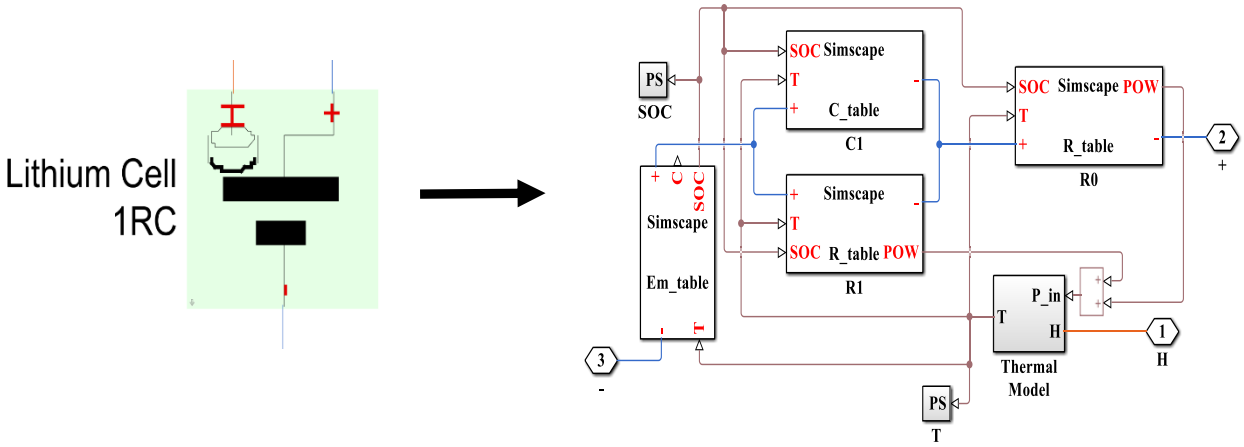

Figure 3.4: 1RC li-Ion Cell overview

After many trials, the following LUT was obtained for the battery components for each set of temperature as shown in figure 3.5 to figure 3.8.

R0 LUT:

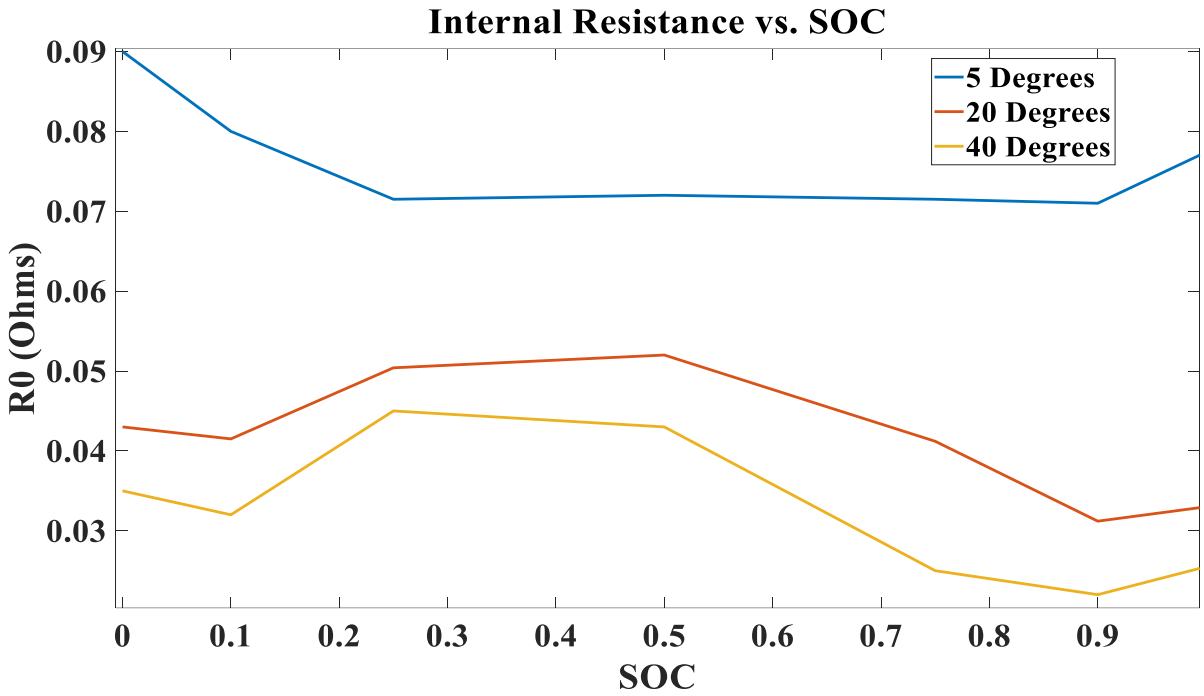

Figure 3.5: Values of R0 vs SOC

R1 LUT:

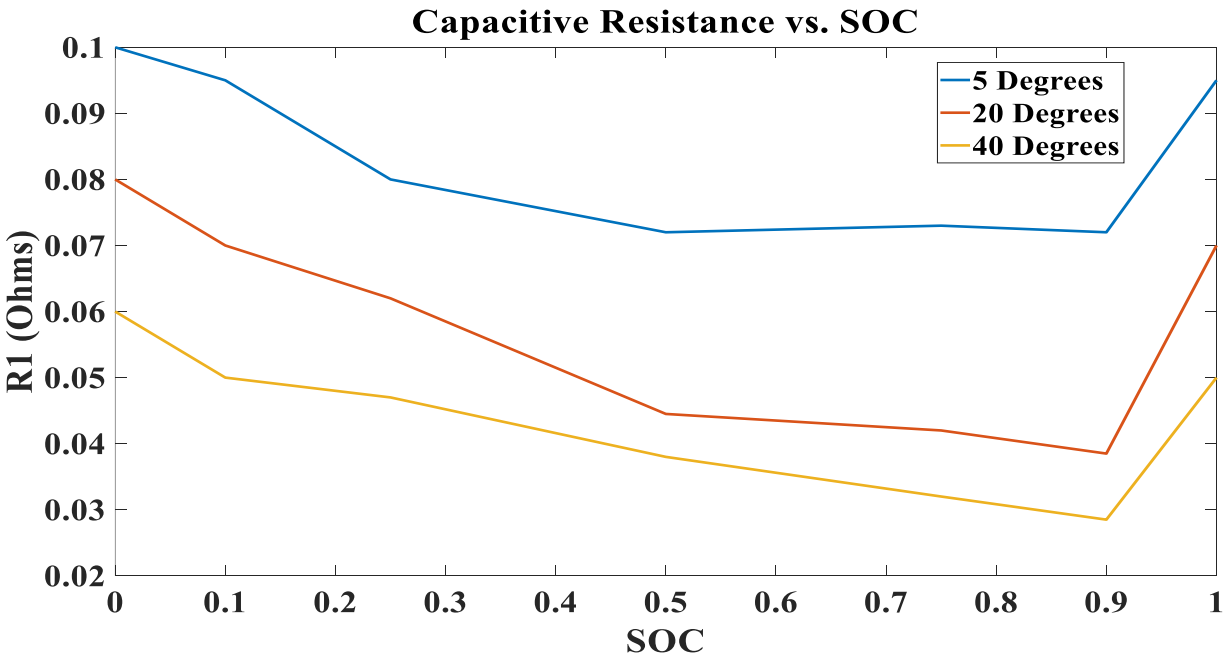

Figure 3.6: Values of R1 vs SOC

C1_LUT:

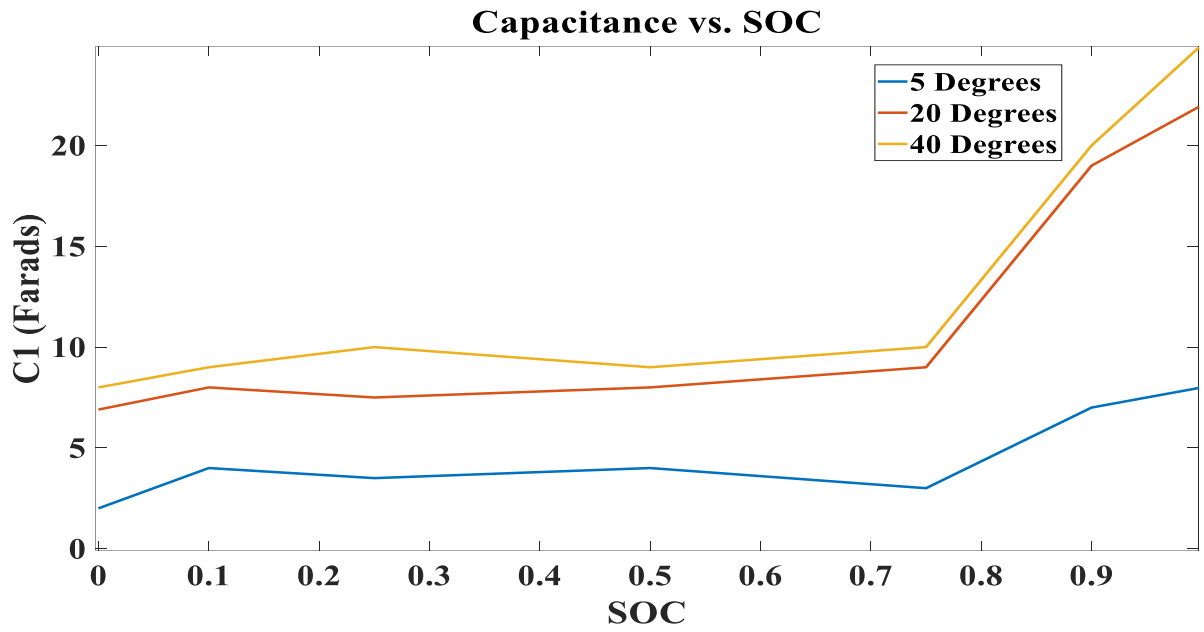

Figure 3.7: Values of C1 vs SOC

Em_LUT:

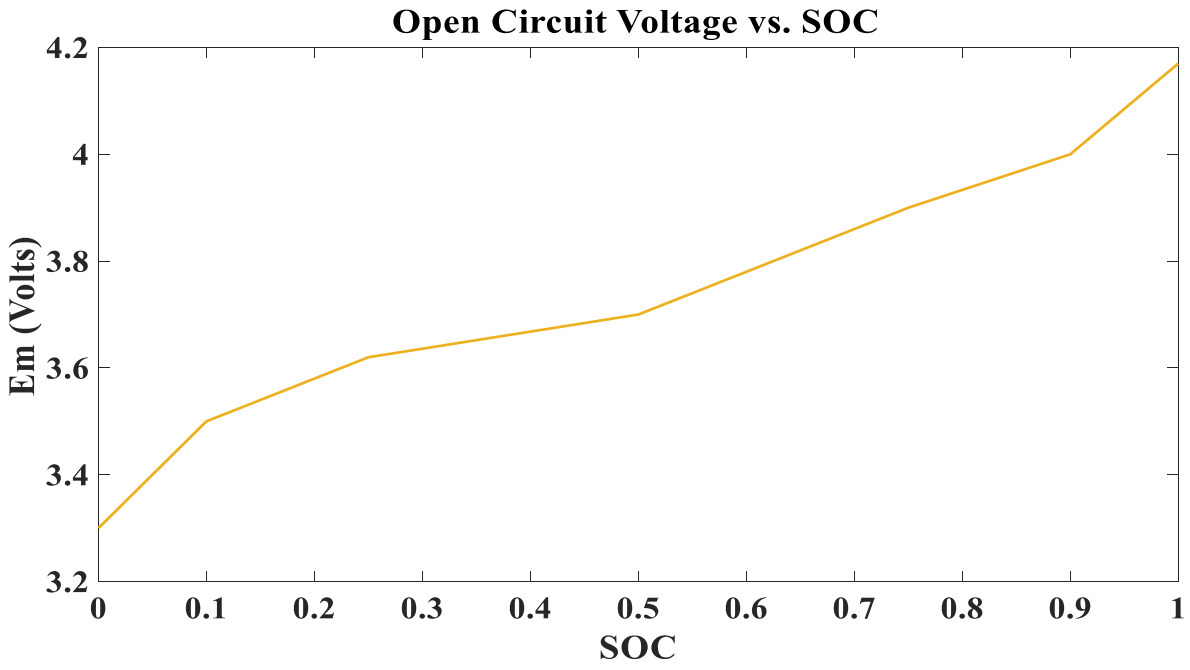

Figure 3.8: Values of C1 vs SOC

3.4 Battery model analysis

3.4.1 Comparison setup for 1RC and 2RC models

In this thesis, we used the 1RC model over the 2RC model to illustrate the effects of charging. This section deals with the difference between the simulation modelling of the 1RC model against the 2RC model of the battery in Simulink and the reason of choosing the 1RC model.

In order to establish the difference, an experimental data of battery discharge was created using a look up table and both the 1RC and 2RC model had the following simulated result (orange) before the parameters were estimated.

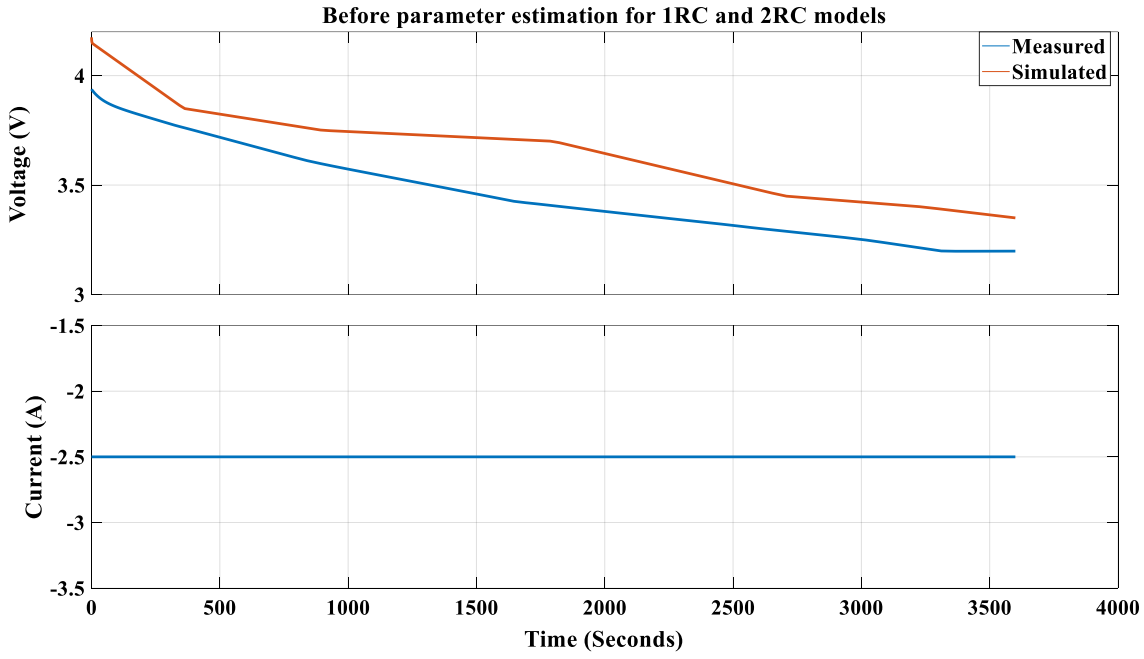

Figure 3.9: Before Parameter estimation for 1RC and 2RC

Figure 3.9 shows that the initial guesses for the parameters of the models are incorrect and require to be estimated to converge the simulated data with the measured data.

3.4.2 1RC model

Figure 3.10 shows the 1RC model of the battery used for parameter estimation. The values of the components Em, R0, R1 and C1 are assigned to a Look up table (LUT). Look up tables allow for more flexibility and ease in changing the parameters to match experimental data.

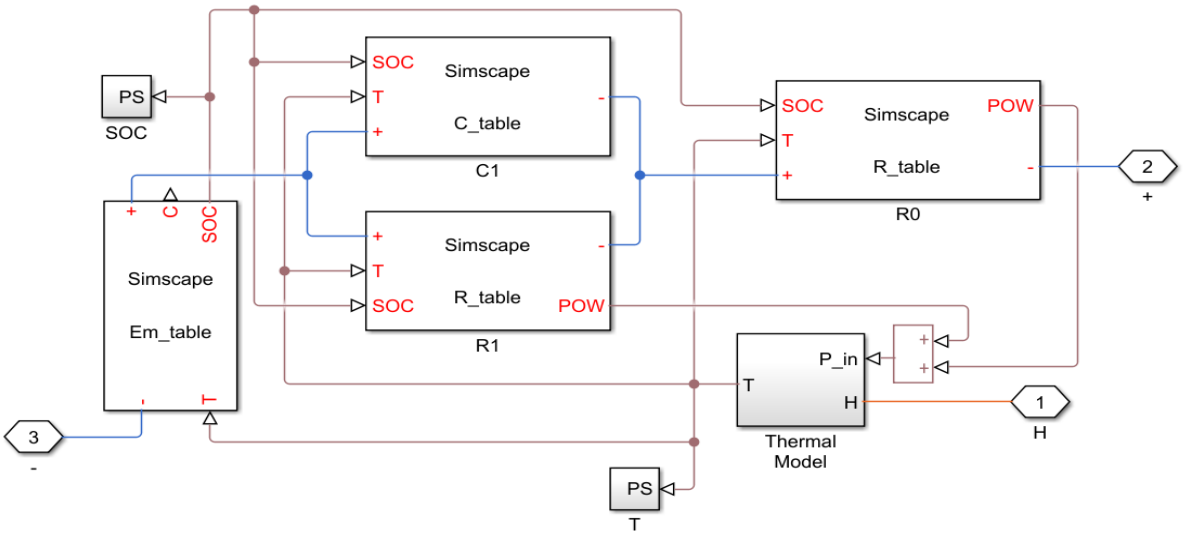

Figure 3.10: 1RC equivalent circuit model

From the figure 3.11 and figure 3.12 shown below, we can observe that the 1RC model was converged very close to the original data, and this was possible after 11 iterations.

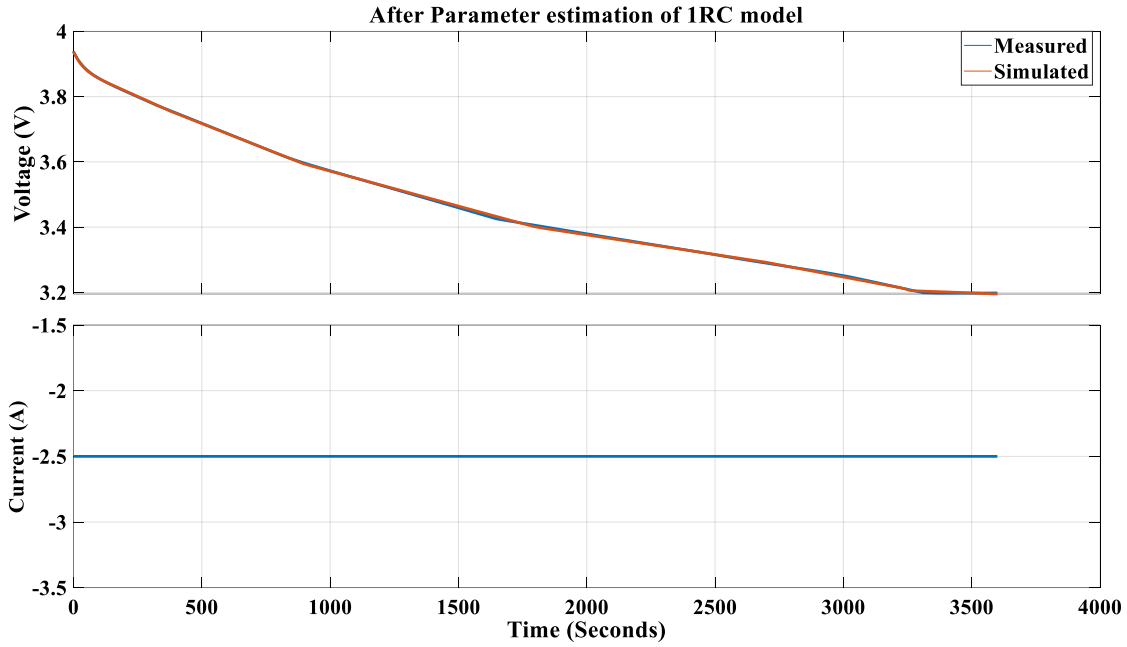

Figure 3.11: Convergence of 1RC model

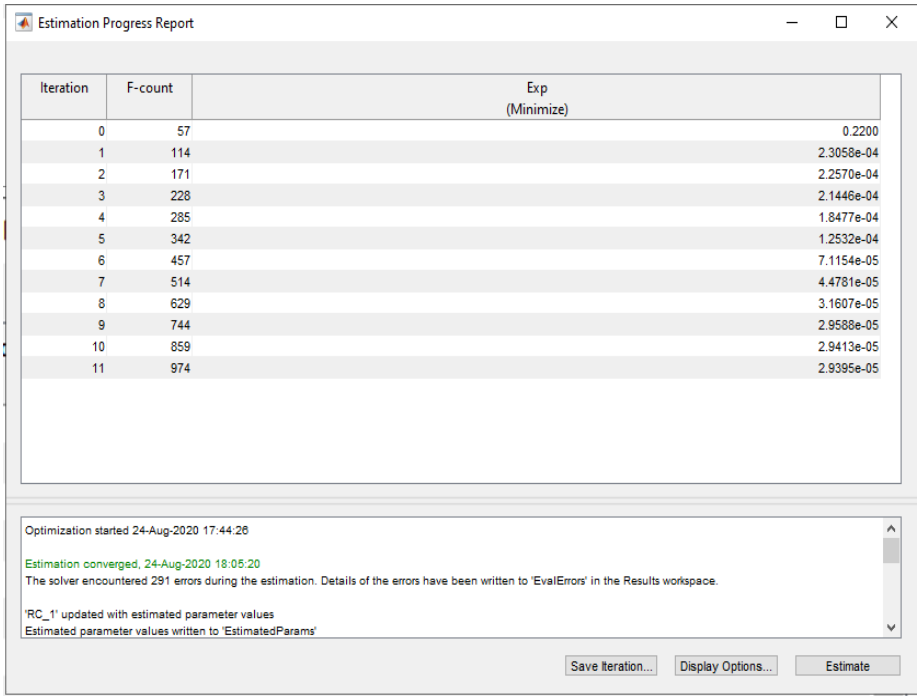

Figure 3.12: Iteration count of estimation for 1RC convergence

The time taken for the 1RC parameter estimation is observed to be around 21 minutes.

3.4.3 2RC model

The 2RC model of the li-Ion battery contains 2 RC branches. This allows for more precise parameter estimation. The model for the 2RC battery circuit elements are shown in figure 3.13

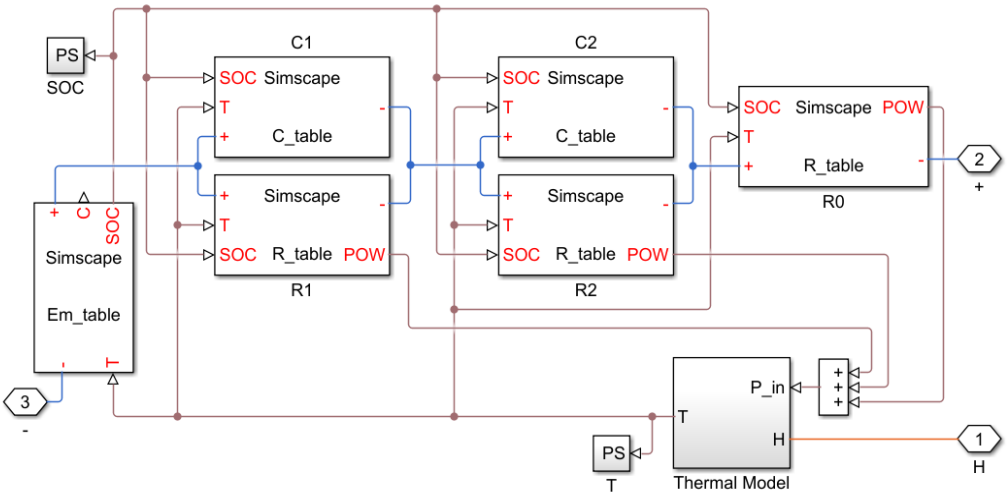

Figure 3.13: 2RC equivalent circuit model

From the figure we can observe that there is an additional R2 and C2 in addition to the elements of the 1RC model, and for each of these elements an extra set of LUT is generated, thereby allowing more room for parameter estimation.

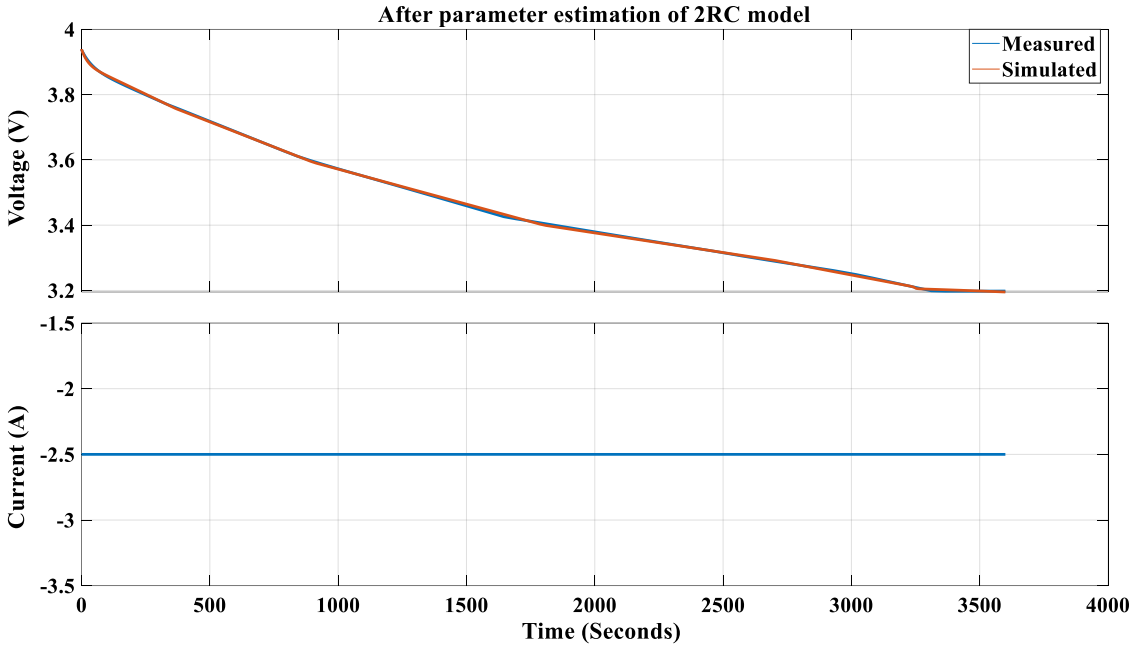

Figure 3.14: Convergence of 2RC model

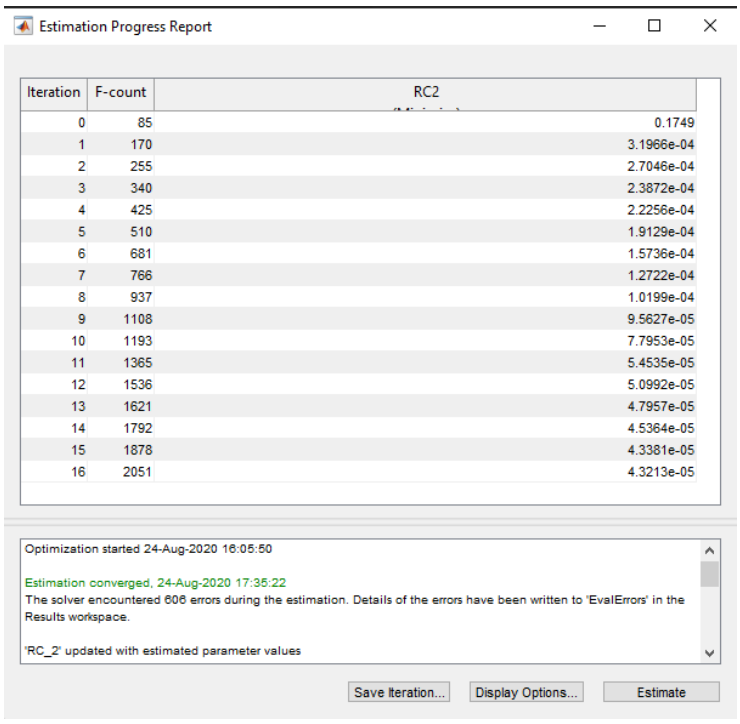

Figure 3.15: Iteration count of estimation for 2RC convergence

Figure 3.14 above shows the convergence of the 2RC model in a similar fashion to the 1RC model. It is observed that to converge the simulated result to the measured data, 16 iterations were required in a time of 1 hour 30 minutes from figure 3.15.

3.4.4 Selection of battery model

The complexity arises with higher RC models due to higher numbers of LUT, which means in order to converge the values of the table to match the experimental data through estimating each component separately, it would be quite difficult as well as extremely time consuming to match the data.

The complexity of 2RC model over the 1RC model is proved in figure 3.15 where the time taken and the iterations conducted by 2RC model to converge the simulated data to the experimental is larger compared to 1RC model in figure 3.12. This is due to the larger number of parameters required to be estimated.

Furthermore, the accuracy of the 2RC model is higher than the 1RC model as it can be observed in **[28].** Here the authors use experimental data to estimate and validate the parameters obtained for the 1RC and 2RC model by running pulsed discharge cycles to match the data obtained. The comparison of the 1RC model with the 2RC model shows that the level of accuracy of 1 RC equivalent circuit model has maximum error in output of 1.64% when compared to 2 RC equivalent circuit models which is 1.22% and the relative output error difference is 0.42%. Thus, this proves that 2RC model is more accurate, yet difficult and more complex to parametrize than the 1RC model. Since the output error of 1RC model is generally quite low, therefore, this thesis uses a 1RC model to maintain the balance between simplicity and accuracy as much as possible considering the complexity of the design of the entire simulation environment.

3.4.5 C-Rate effect on polarization

The Effects of various amplitudes of charging current (C-rates) on the battery model has been provided, which is a vital concept for the proposed design in this thesis.

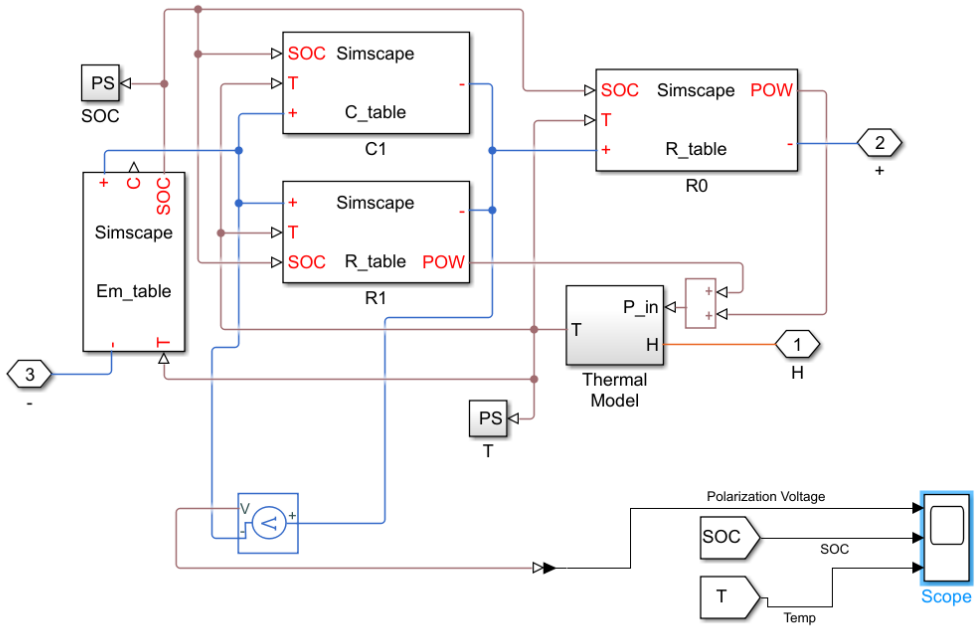

Figure 3.16: Measuring effect of C-rates on 1RC model

The figure 3.16 above shows the inside of the cell model used to measure the polarization voltage, temperature and SOC by connecting a voltage sensor across the RC branch, connecting the temperature signal and SOC signal to the Scope respectively.

The current supplied to the battery is set at different Current values and the effects on the polarization voltage of the battery against SOC is illustrated in the graph below:

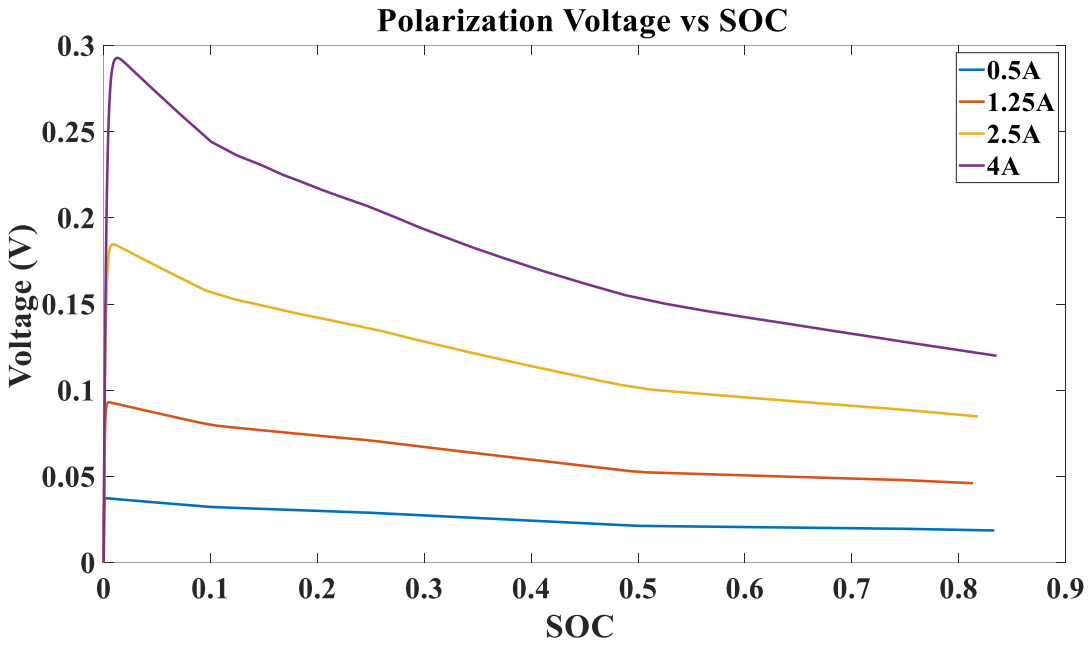

Figure 3.17: Effect on polarization at different C-rates

The following graph shows the temperature rise with respect to SOC with various Currents:

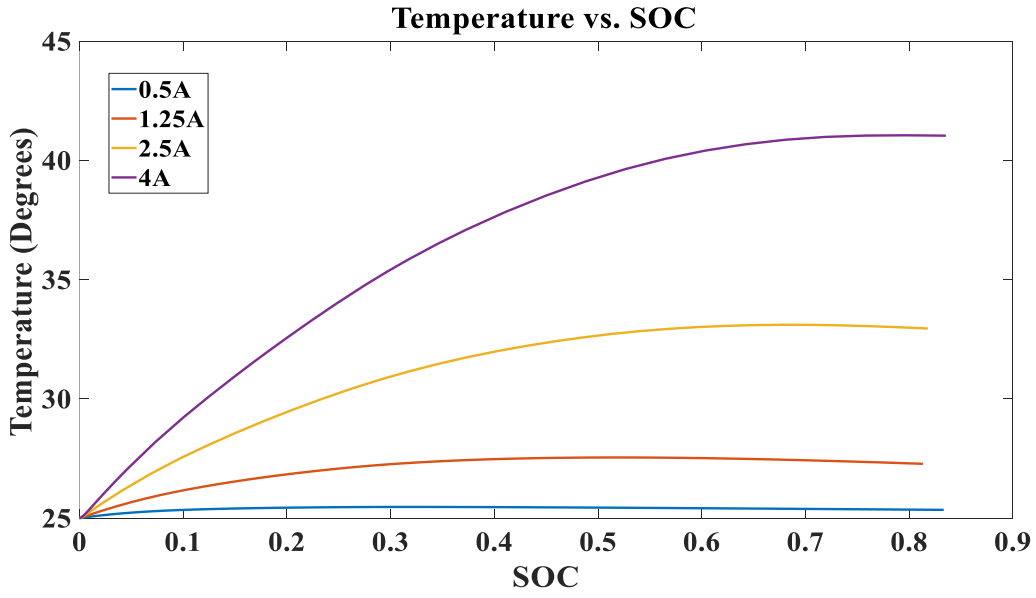

Figure 3.18: Effect on temperature at different C-rates

Figure 3.17 and figure 3.18 show that at higher C-rates, the polarization voltage is very high and this leads to higher temperature within the battery. The effects of Current on polarization has also been shown through experiments in **[17]** which also show similar effect of increasing current on polarization and temperature.

3.4.6 Frequency vs charging current

The developed model was tested to show the effects of changing frequencies from 0.1Hz to 10Hz at different SOC values of 20, 40, 60 and 80 percent. The test was done using the simulation battery model by setting the charging voltage at 4.2V and applying a duty cycle of 50 percent in each case, while the frequency control gain block was changed. The following figure 3.19 shows how the simulation test was performed:

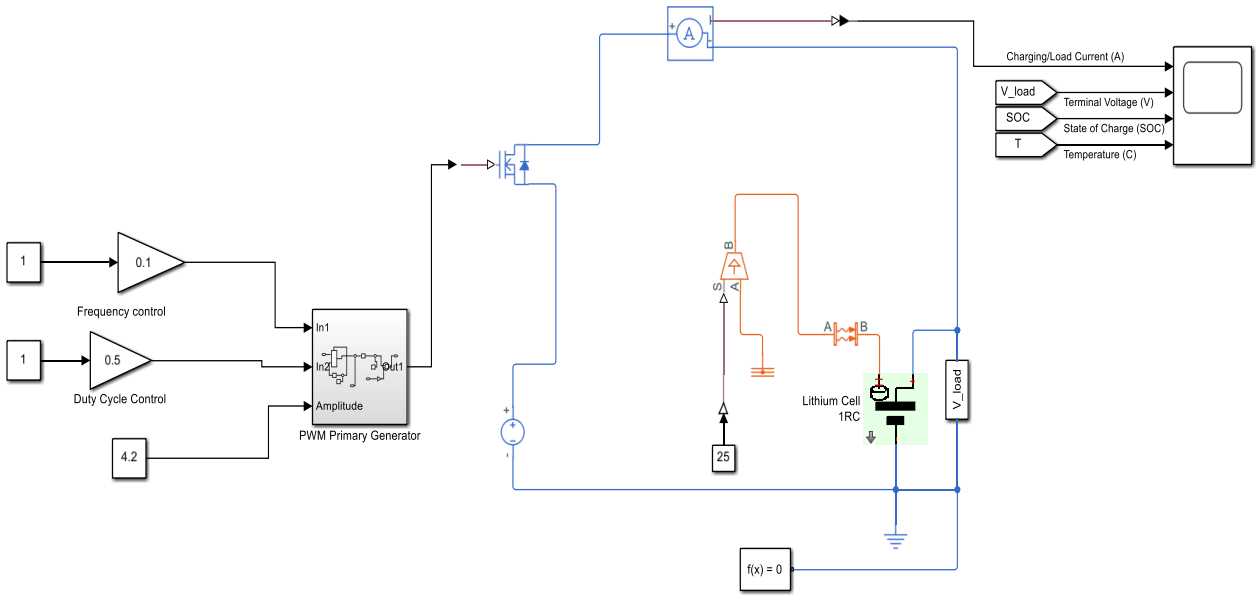

Figure 3.19: Measuring effect of frequency on 1RC model

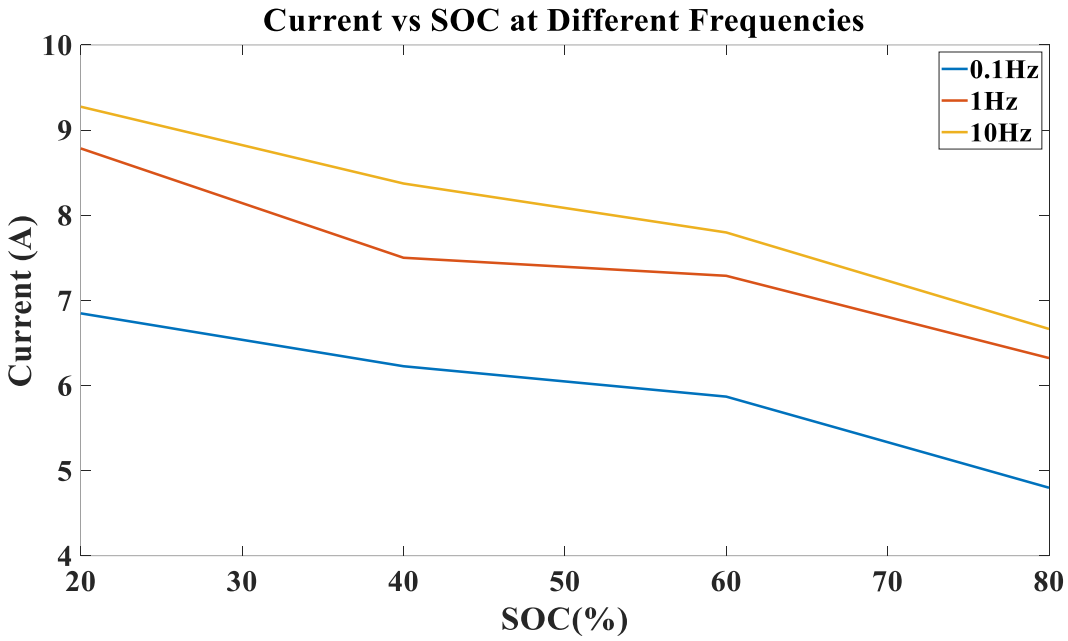

Figure 3.20: Effect on available maximum current at different Frequencies

From figure 3.20 above we can observe that a higher frequency tends to allow higher current injection as the overall impedance of the battery decreases which is proved in **[14]** where the authors measured the impedance of the battery at various frequencies using Solartron 1280 analyzer. However, the experiment using the Solartron 1280 analyzer shows that at very high frequencies, the impedance starts to rise due to battery internal chemistry, but this effect is not possible to be implemented in the 1RC model in Simulink as the battery model responds according to equation 6, thus a higher frequency will reduce the impedance.

3.5 Simulation outputs and results

Using the mentioned LUT values for each component, the charging current, Average current, Temperature, Terminal Voltage and SOC graphs were obtained after running the simulation. They are as follows:

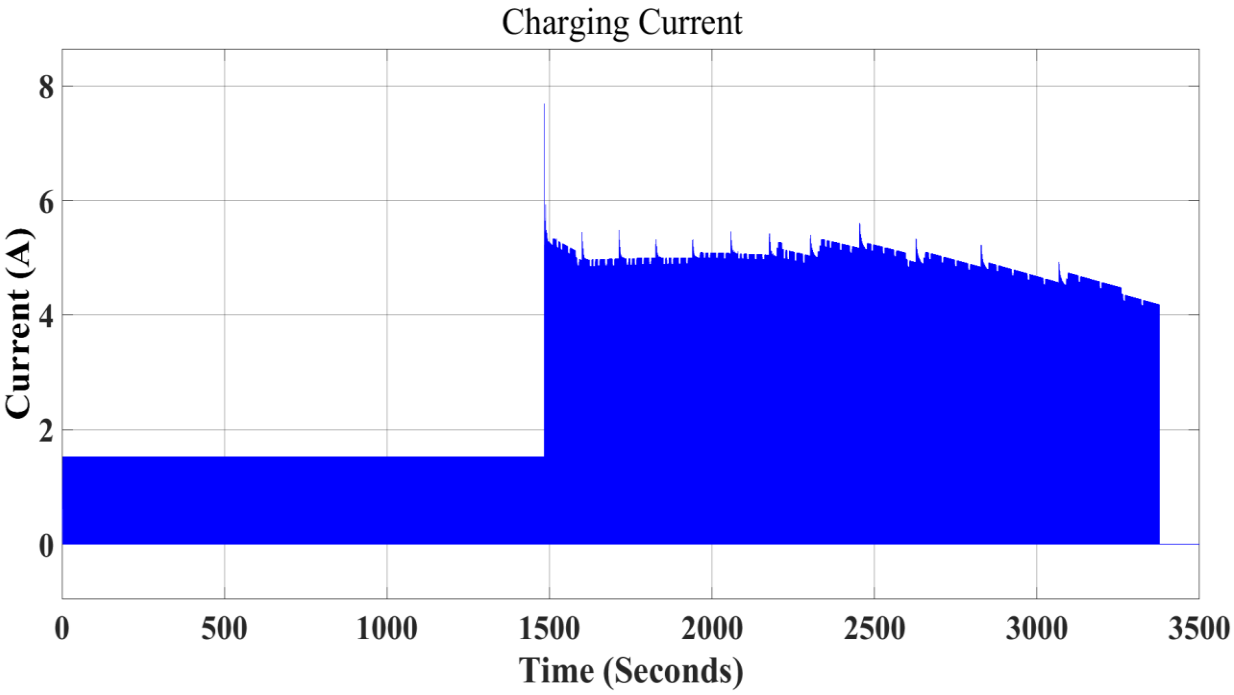

Figure 3.21: Charging current of the Battery

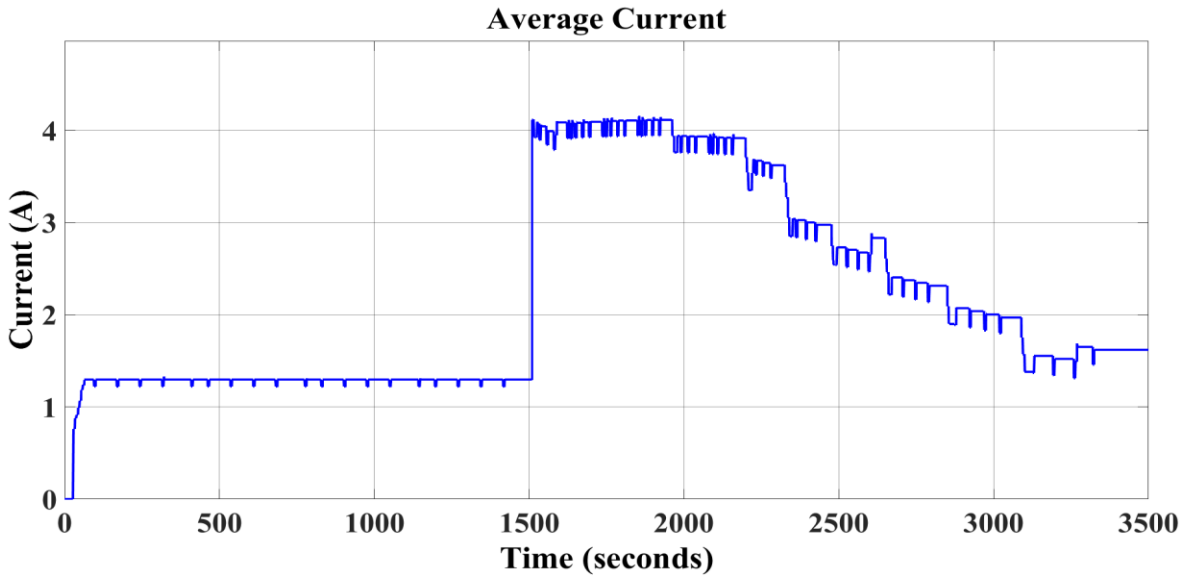

Figure 3.22: Average Current against Time during charging

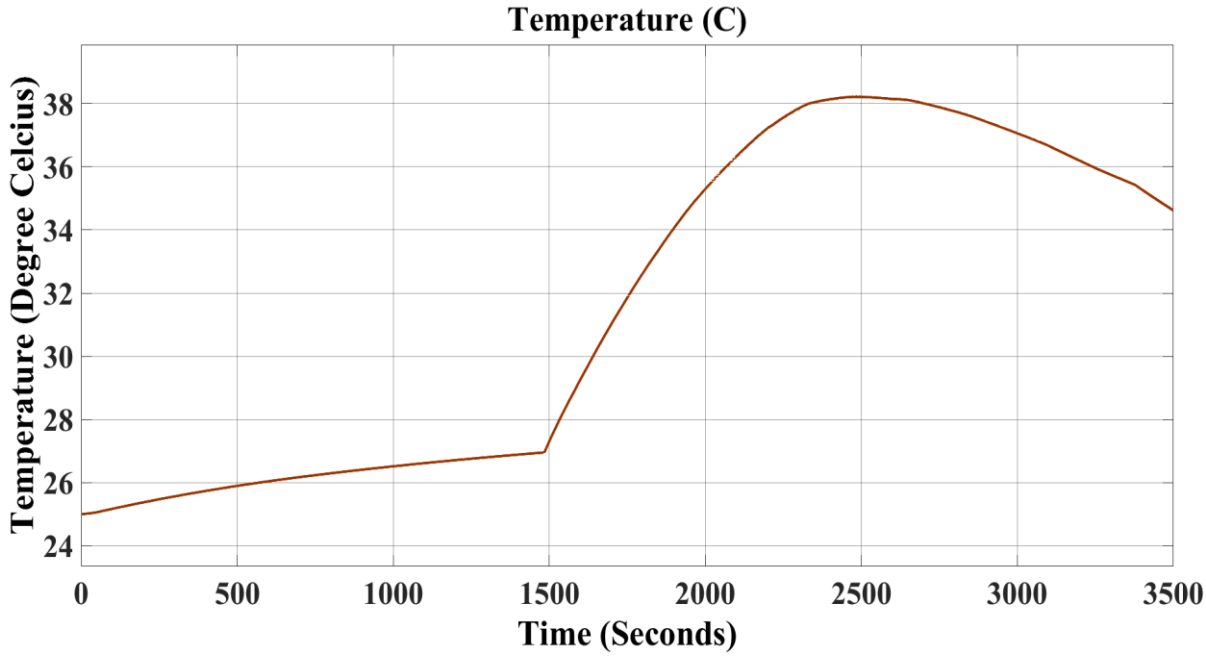

Figure 3.23: Temperature against time during charging

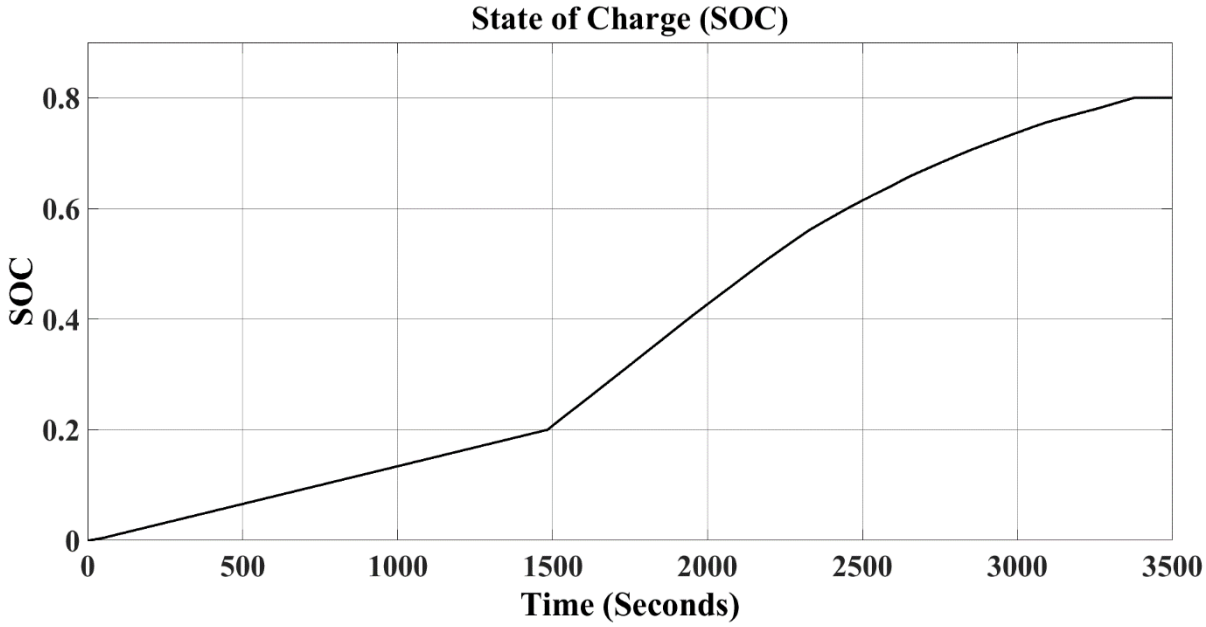

Figure 3.24: SOC against Time during charging

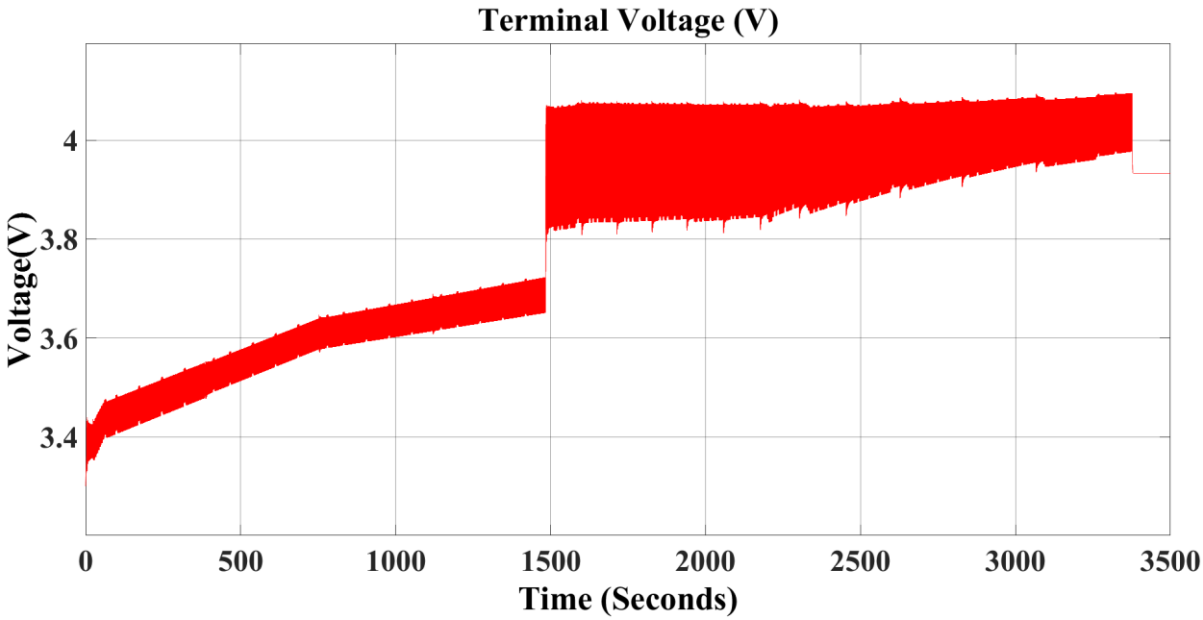

Figure 3.25: Terminal Voltage against time during charging

Figure 3.21 represents the charging current injected into the battery, for the first 1500 seconds, it is observed that the maximum current is 1.5A, and rises to around 5A after 1500 seconds. However, the average current is manipulated via the duty cycle and frequency gain blocks through the charge controller and is maintained within the boundaries as observed in figure 3.22.

Figure 3.23 shows the temperature curve which rises steadily until 20 percent SOC and then sharply rises as the charge current goes from 1.25A to 4A, but then becomes steady and slowly declines as the charging current is lowered at higher SOC values.

Figure 3.24 shows the rise of State of charge (SOC) as the battery is charged, showing that the rise is steady from 0 to 20 percent SOC during the first 1500 seconds due to the low current input, and rises abruptly afterwards as a larger current is injected.

Figure 3.25 is the battery terminal voltage, at first it remains low to limit the current to 1.5A by keeping the difference between the charging voltage and the battery voltage low enough,

after 1500 seconds the terminal voltage rises greatly, thereby raising the charging current across the battery.

From the above figures, it can be seen that the charge time takes 3380 seconds which is approximately 56 minutes and the temperature rise of the battery is also from 25 to 38 degrees.

Furthermore, the following figure 3.26 and figure 3.27 shows how the frequency and duty cycle are controlled during the charging process by the charge controller:

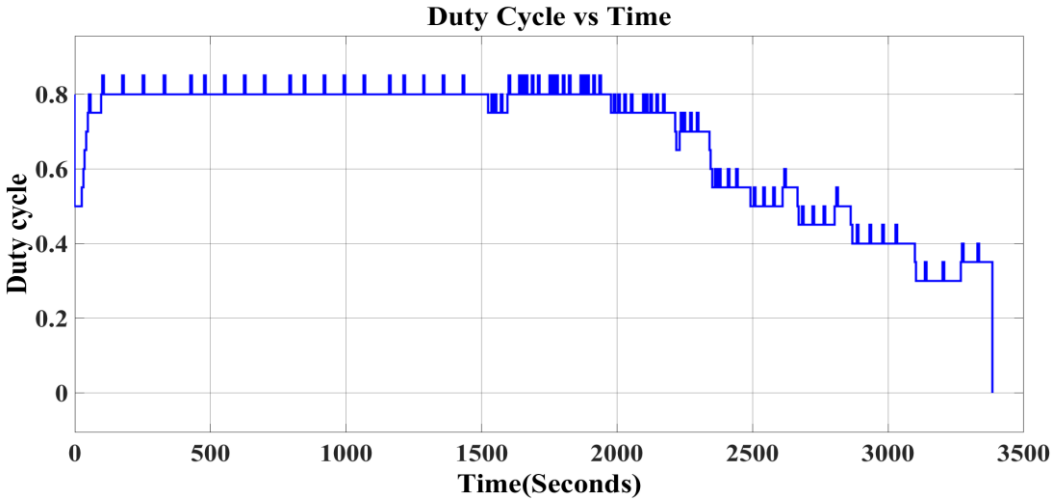

Figure 3.26: Duty cycle charging process

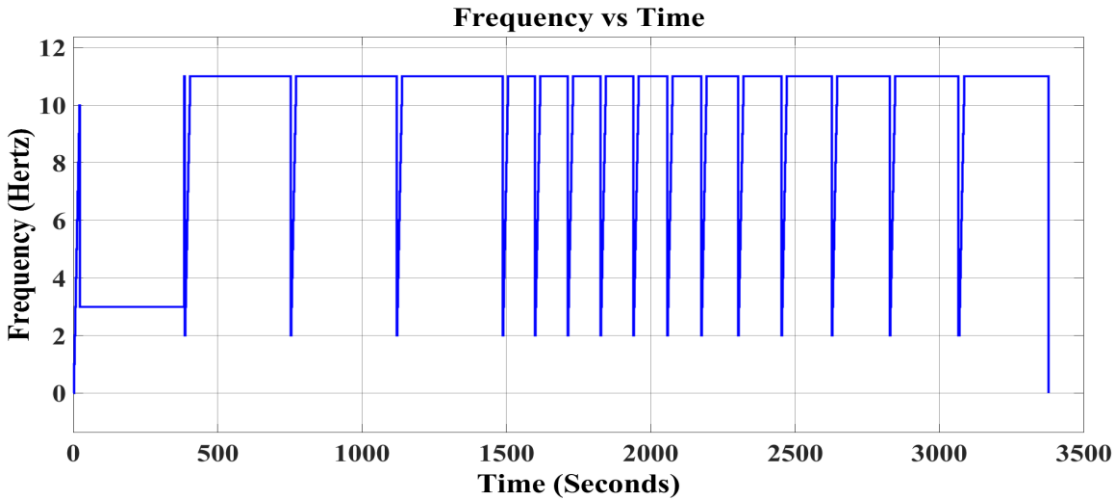

Figure 3.27: Frequency during charging process

The duty cycle is around 80 percent in the first 1500 seconds as the injected current is low, but after 1500 seconds, as the input current is very high, the duty cycle is slowly lowered to maintain the average current to prevent overheating of the battery. Furthermore, it can be observed that the frequency is selected as 11Hz for the most of the time as a higher frequency allows for minimum impedance of the battery.

3.6 SPCS drawbacks

Despite the SPCS being a fast and reliable method, it still possesses a few drawbacks. The current state of this system allows for charging time of 56 minutes with a temperature rise of 13.3 degrees. However, trying to reduce the time of charging would require either to raise the current amplitude or to increase the duty cycle, either of which would lead to a high polarization and high temperature rise. As a result, continuous high polarization and high temperatures would eventually lead to premature degradation of the battery and would highly impact its lifetime. Therefore, a different approach known as the double pulse charging system has been implemented to reduce the effects of raised polarization and temperature while reducing the time of charging the batteries as explained in the next chapter.

3.7 Conclusion

This chapter clearly shows the single pulse charging system implementation and that the simulation outputs are similar to previous works. The charging time taken in the SPCS method is 56 minutes and the temperature rose by 13.3 degrees. Regardless of being much faster than other methods available in the markets, it still requires a very long time to charge and further improvements in charge time are still a high demand. Unfortunately, due to the high amount of polarization and temperature effects for larger currents and duty cycles, this method still lacks the ability to charge a battery any faster. Therefore, the next chapter deals with the double pulse charging system (DPCS) strategy to overcome the mentioned issues.

Chapter 4: Double Pulse Charging System (DPCS)

4.1 Introduction

In this chapter we introduce our proposed method known as the Double Pulse Charging System (DPCS). Here we show and explain the implementation of such a system in Simulink. The outputs and results of using this system by changing different parameters are also discussed later in the paper followed by the use of current limiting technique. Altogether this technique modifies the SPCS and provides for a more optimal solution, which is shown and compared with other previous literatures to prove the effectiveness of our proposed method.

4.2 Secondary pulse generator design

The following figure 4.1 and figure 4.2 illustrate the design of the secondary PWM generator required to implement the secondary low amplitude current pulses to the battery.

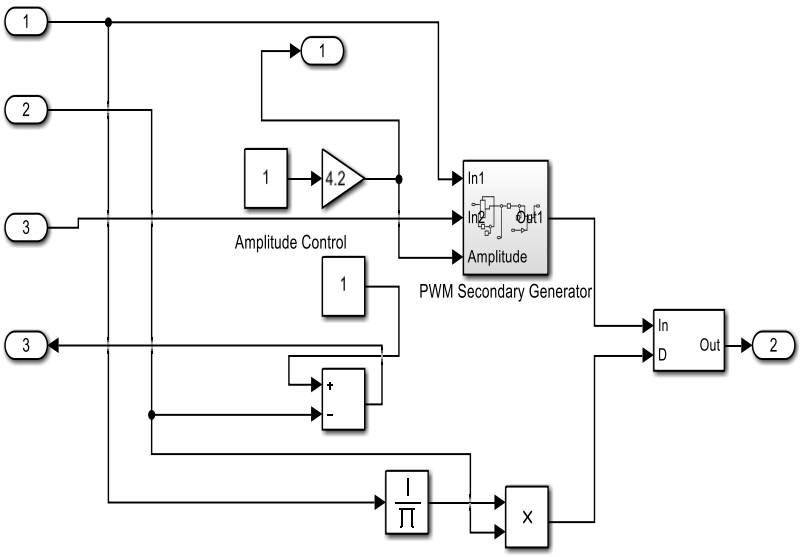

Figure 4.1: Secondary PWM Generator Design

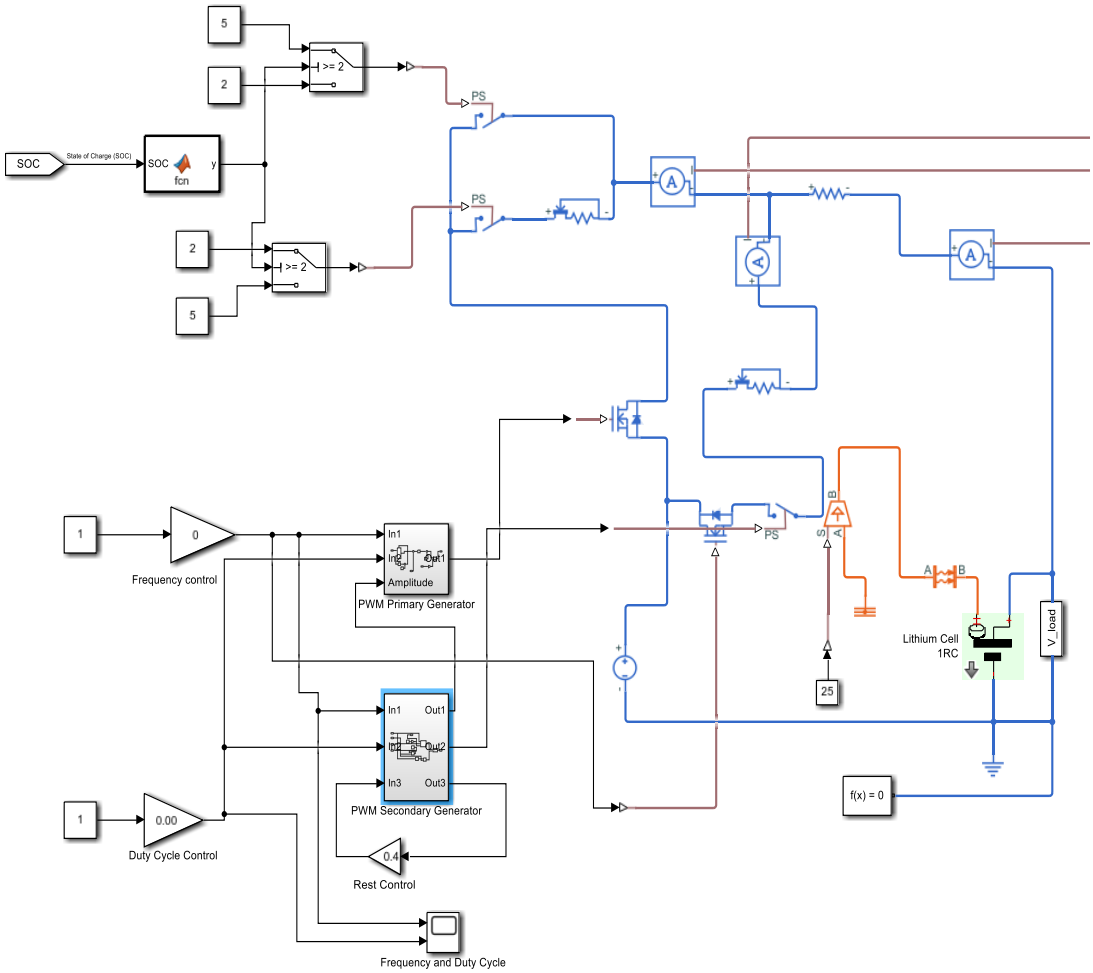

Figure 4.2: DPCS Implementation

The secondary pulse generator in figure 4.1 provides the low amplitude secondary pulse alongside the primary PWM generator which was initially used for battery charging. The secondary PWM generator manipulates the resting period of the primary PWM by applying a small current during those resting periods. The duty cycle of the secondary pulse determines what percentage of the resting period is to be used for the injection of the smaller current pulse. The implementation of the both PWM generators together in action are shown in figure 4.2. As a result, with the help of secondary pulse it is now possible to implement overall larger average current and thus reducing the charging time without contributing much to the heat or polarization of the battery.

For the Secondary Pulse, the frequency is the same as that of the primary pulse generator but the duty cycle is changed according to user's desire by changing the 'rest control' gain block. To achieve this, a subtract block is used to subtract the duty of the primary pulse generator from 1 and is represented by equation 12.

$$Ds'=(1-Dp) \tag{12}$$

where Dp is the duty cycle of the Primary generator and Ds' is the rest period of the primary pulse. For example, a duty cycle of 30% time is followed by a resting period of 70% for the primary pulse generator. To obtain the percentage of the rest period, the ON period has to be subtracted from the entire period as shown in equation 13.

$$Ds'= (1-0.3) = 0.7 \tag{13}$$

However, in order to manipulate the percentage of the resting period for which the secondary pulse will remain ON, the 'Rest control' gain block comes into play, thus the new equation stands as given in equation 14.

$$Ds= Ds' * G_{ON} \tag{14}$$

Where G_{ON} Refers to the desired percentage of the rest period from 0 to 1.

An issue that was encountered was the output of secondary pulse started from the initial position of the primary pulse instead of the resting period. To solve this a delay block was implemented. The input of the delay block used a Reciprocal block (1/f) first to get the period from frequency(f) which was multiplied with the duty cycle (Dp). The output of the time delay block was then sent towards the Final output. The input of the delay block can be mathematically expressed as provided by equation 15.

$$Delay= 1/Fp * Dp \tag{15}$$

4.3 Simulation and results

The effect of adding a secondary pulse width generator to produce secondary pulses during the rest period of the primary pulses are shown in figure 4.3 and figure 4.4

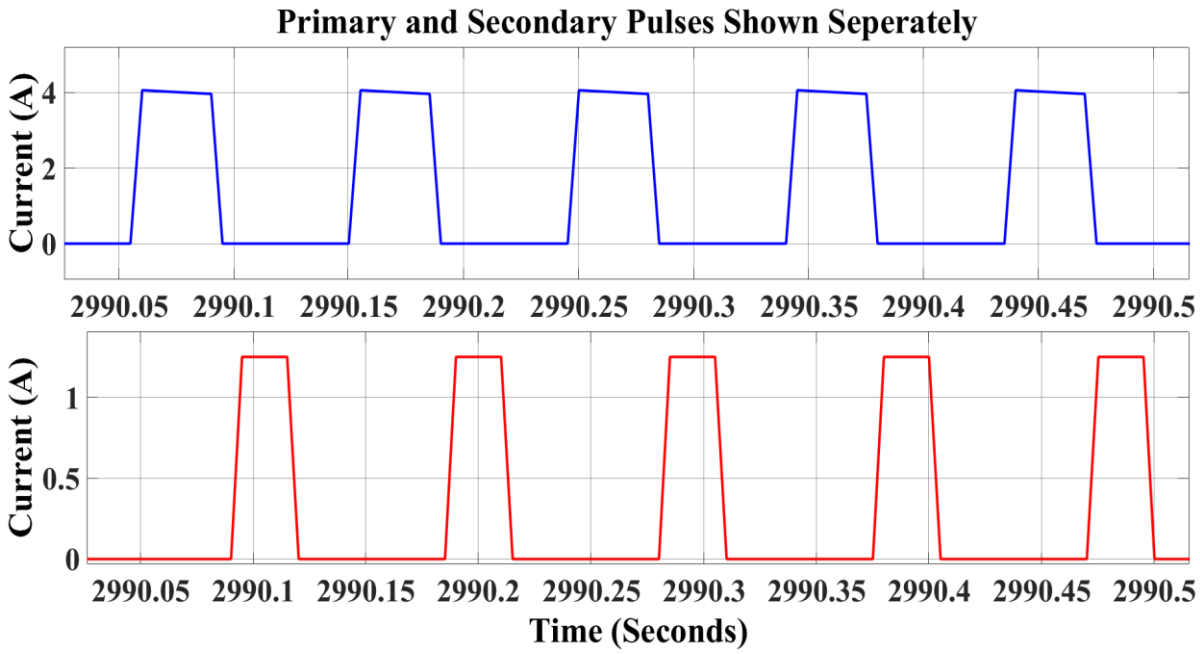

Figure 4.3: Primary and secondary pulses in separate windows

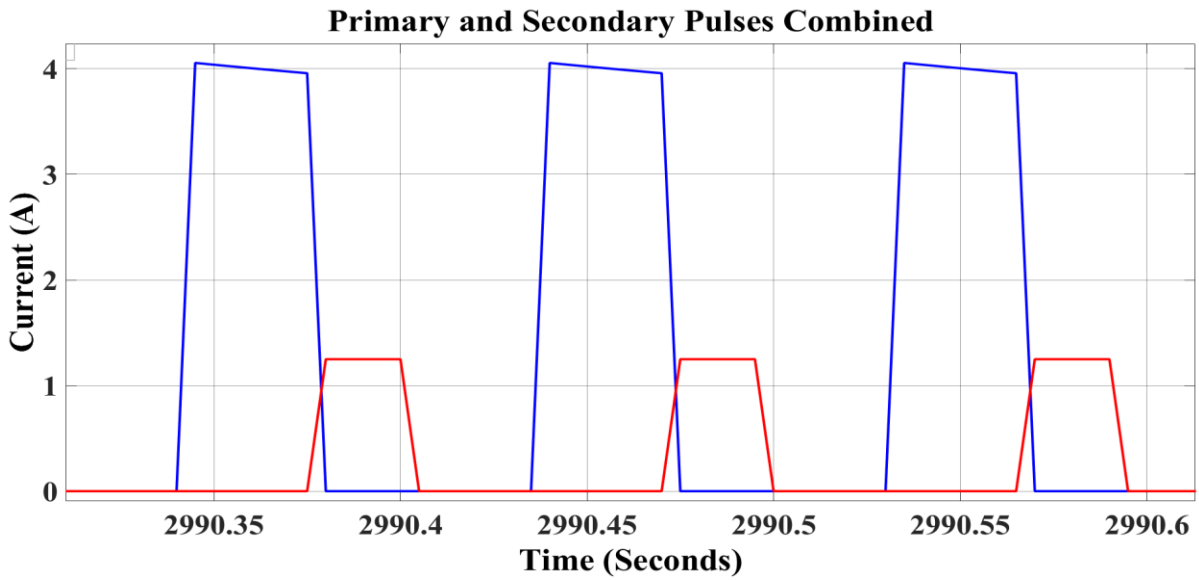

Figure 4.4: Primary and secondary pulses combined

Figure 4.3 displays the primary and secondary pulse output in different windows, while figure 4.4 displays both the primary pulse generator output and the secondary pulse generator output working together. The primary current (blue) injected into the battery is approximately 4.5A with a period of 0.1s. The primary pulse is ON for 0.04 seconds and has a resting time of 0.06 seconds. The secondary pulse has (red) an amplitude of 1.25A and has an ON time of 0.024s, which is 40% of the rest period of the primary pulse.

4.4 Results of varying duty cycle on secondary pulse

4.4.1 Results obtained without current limiter

Table 4.1 shows the results of the simulation runs using various C-rates for different duty cycles of the Secondary Pulse. The time taken to charge and the temperature rise are recorded seperately for each case.

ON time		10%	25%	50%	75%	90%	100%
0.25A (0.1C)	**Time (sec)**	3331	3317	3281.26	3245.38	3216.22	3202.35
	Temperature rise (°C)	38.3	38.3	38.3	38.3	38.3	38.3
0.83A (1/3C)	**Time (sec)**	3245.9	3188.01	3094.77	2994.4	2929.8	2915.46
	Temperature rise (°C)	38.3	38.4	38.4	38.5	38.5	38.5
1.25A (0.5C)	**Time (sec)**	3173.65	3109.1	2972.86	2843.75	2764.86	2736.18
	Temperature rise (°C)	38.4	38.5	38.5	38.7	38.8	38.8
2.5A (1C)	**Time (sec)**	2945.19	2842.27	2636.49	2453.13	2361.82	2342.88
	Temperature rise (°C)	39.1	39.2	39.5	39.8	40	40
3A (1.2C)	**Time (sec)**	2951.33	2822.22	2571.22	2370.39	2269.97	2241.28
	Temperature rise (°C)	38.8	39	39.5	40	40.2	40.3
4A (1.6C)	**Time (sec)**	2836.23	2693.13	2420.58	2212.61	2115.02	2083.5
	Temperature rise(° C)	39.2	39.5	40.2	40.7	41.1	41.2

Table 4.1: Time and Temperature reading on different DC. (Double Pulse Charging (DPC) Method)

From the table, we get the minimum charging time as **2083.497 seconds** and maximum temperature **41.2° C** for a maximum current amplitude of 4A at 100 percent DC while the

maximum charging time occurs at **3331 seconds** for a temperature rise of **38.3° C** degrees compared to the **single pulse method** where the Temperature rise was **38.3° C** and Charging Time was **3373 seconds.**

For our used battery model, the maximum temperature can be raised to 45(degree Celsius). But it is recommended for better battery life we keep the temperature within 40° C. The results obtained indicate that for a faster charging time a higher current value and DC is much more preferred, however at the cost of high rise in temperature. As discussed earlier, a higher current value means a higher voltage polarization which would lead to higher temperatures and cause battery damage. Hence, a balance between fast charging time and low temperature rise is essential.

4.4.2 Results obtained after adding an extra current limiter:

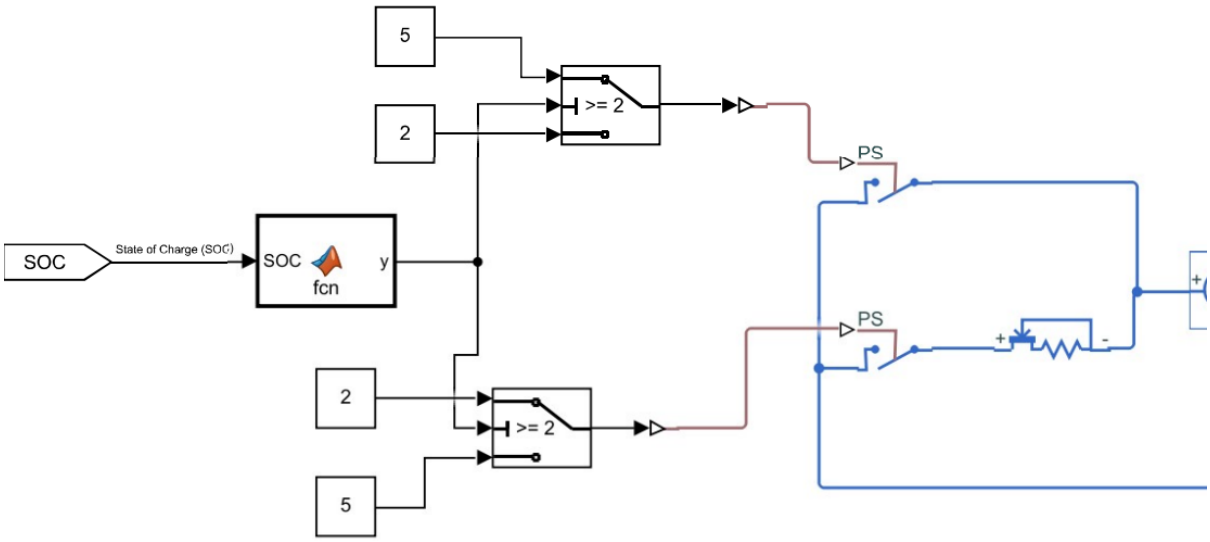

Figure 4.5: DPCS without current limiter at upper channel

One final modification has been done to improve the charging time in a moderate temperature rise. Now, to control the polarization of the battery more efficiently while SOC exceed first

20%, an extra current limiter has been used in the upper line of the switches. Here, an extra current limiter is added like in Figure 4.6 so that the amplitude of the primary current can be limited.

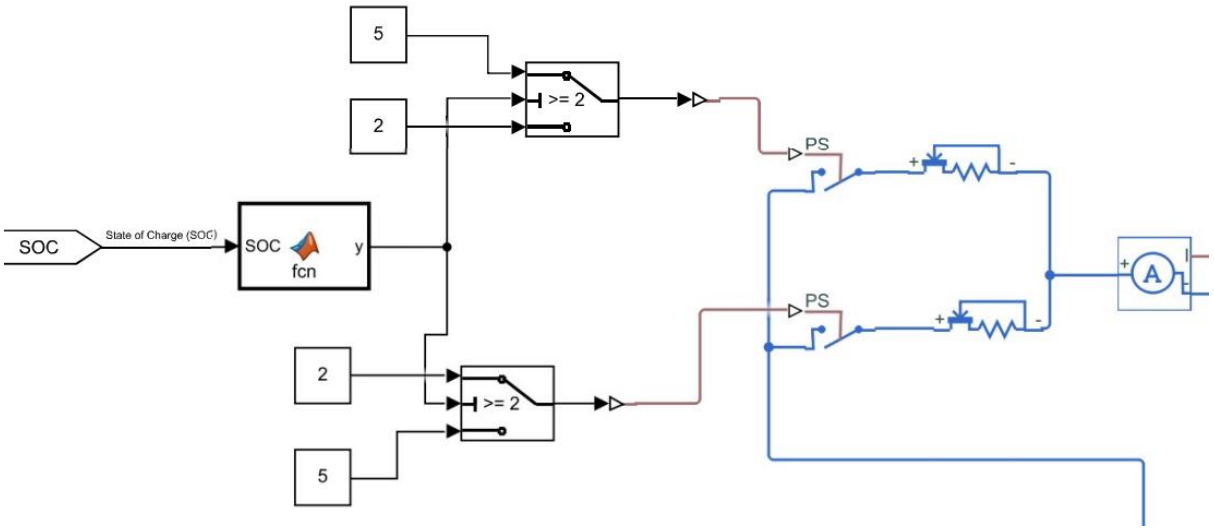

Figure 4.6: DPCS with current limiter in upper channel

Table 4.2 shows a second set of data extracted using a current limiter in Figure 4.6 to limit the amplitude of the primary charging current, as it has been observed that higher injection current is responsible for higher values of polarization leading to higher temperatures. As a result, it is observed that the temperature rise decreases by about 1 degree compared to that found in the previous simulation without the current limiter. This is much favorable for the battery, however a slight rise in charging time is also observed due to the fact that the extra current limiter has a voltage drop across it, thereby leading to a fall in overall charging current in the final charging stage.

ON time		10%	25%	50%	75%	90%	100%
0.25A (0.1C)	Time(sec)	3321.51	3319.62	3281.99	3257.24	3232.14	3219.73
	Temp rise (°C)	37.4	37.4	37.5	37.5	37.5	37.5
0.83A (1/3C)	Time(sec)	3232.14	3194.92	3095.20	3008.01	2958.16	2933.07
	Temp rise (°C)	37.6	37.6	37.6	37.7	37.7	37.7
1.25A(0.5C)	Time(sec)	3157.49	3107.78	2983.18	2870.99	2796.24	2783.58
	Temp rise (°C)	37.6	37.7	37.8	37.8	37.9	38
2.5A(1C)	Time(sec)	2999.32	2906.91	2711.15	2538.42	2458.01	2423.41
	Temp rise (°C)	38	38	38.3	38.5	38.7	38.8
3A(1.2C)	Time(sec)	2932.98	2833.65	2609.27	2435.05	2347.97	2322.93
	Temp rise (°C)	38.1	38.2	38.6	38.9	39.1	39.2
4A(1.6C)	Time(sec)	2833.61	2721.61	2472.40	2298.02	2198.37	2170.21
	Temp rise (°C)	38.4	38.6	39.2	39.6	39.9	40

Table 4.2: Time and Temperature reading on different duty cycles using Current limiter.

(DPC Method)

From the Table 4.2, we get the minimum charging time as **2170.213 seconds** and maximum temperature **40° C** for a maximum current amplitude of 4A at 100 percent duty cycle while the maximum charging time occurs at **3321.511 seconds** for a temperature rise of **37.4° C** degrees compared to the **without this extra CL in 4.3.1** where the min Temperature rise was **38.3° C** and Charging Time was **3331 seconds.**

4.5 Result analysis

4.5.1 Result analysis without the extra current limiter

In Figure 4.7, graphical representation of Table 4.1 is presented for better understanding. In this Temperature (°C) vs. Time (sec) graph, Duty Cycle (% DC) series for 4A (green one) are labeled and for other currents (3A, 2.5A, 1.25A, 0.83A & 0.25A) the sequences are same (100% to 10%: From left to Right).

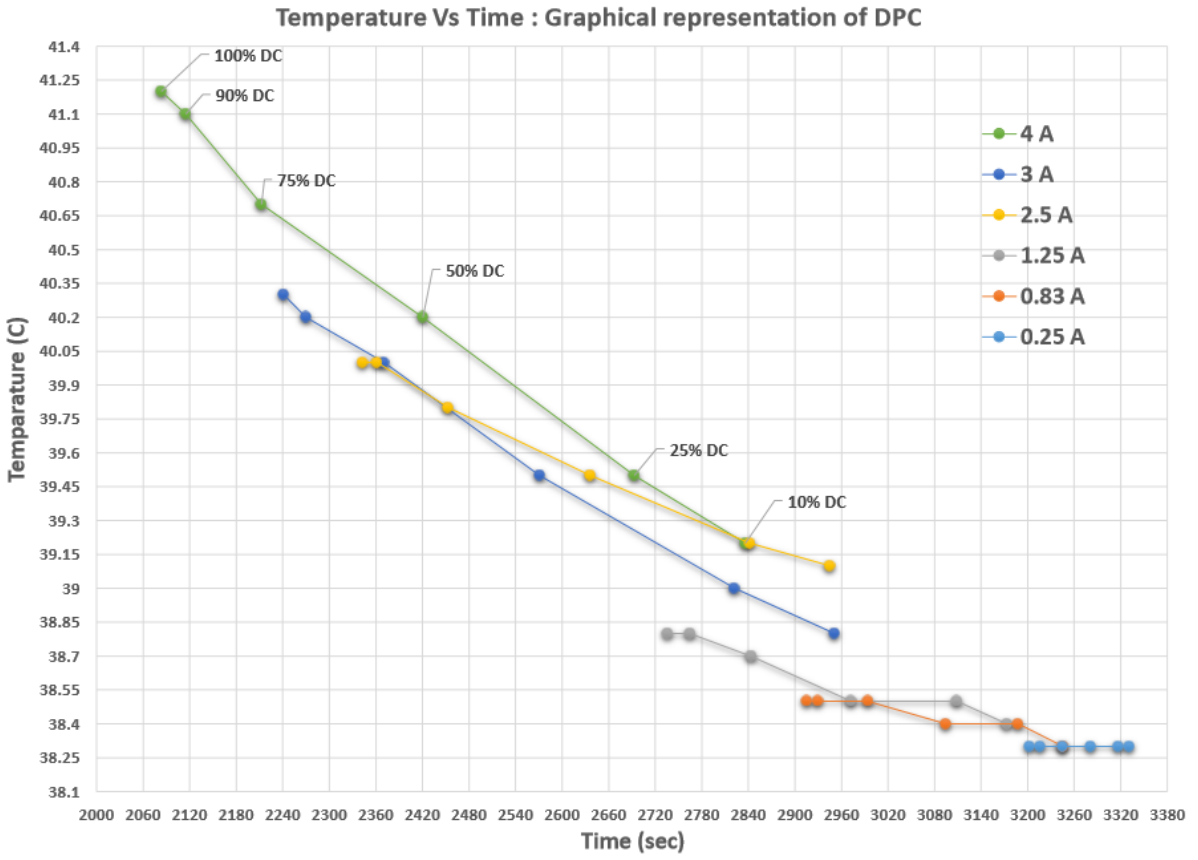

Figure 4.7: Temperature Vs. Time (Graphical Representation of Table 2)

From the Figure 4.7, it can be observed that in most cases for any current, the maximum Temperature is found in maximum DC (100%). So, it can be said that here Temperature is changing proportionally with the DC with respect to any current.

Temperature α Duty Cycle

And if it is observed from the charging time's perspective, it can be said that the charging time is inversely proportional to the both Temperature and DC.

$$\textbf{Charging Time } \alpha \ \frac{1}{\textbf{Duty Cycle}}$$

$$\textbf{Charging Time } \alpha \ \frac{1}{\textbf{Temperature}}$$

4.5.2 Result analysis using an extra current limiter

In Figure 4.8, graphical representation of Table 4.2 is presented for better understanding. In this Temperature (°C) vs. Time (sec) graph, Duty Cycle (% DC) series for 4A (green one) are labeled and for other currents (3A, 2.5A, 1.25A, 0.83A & 0.25A) the sequences are same (100% to 10%: From left to Right).

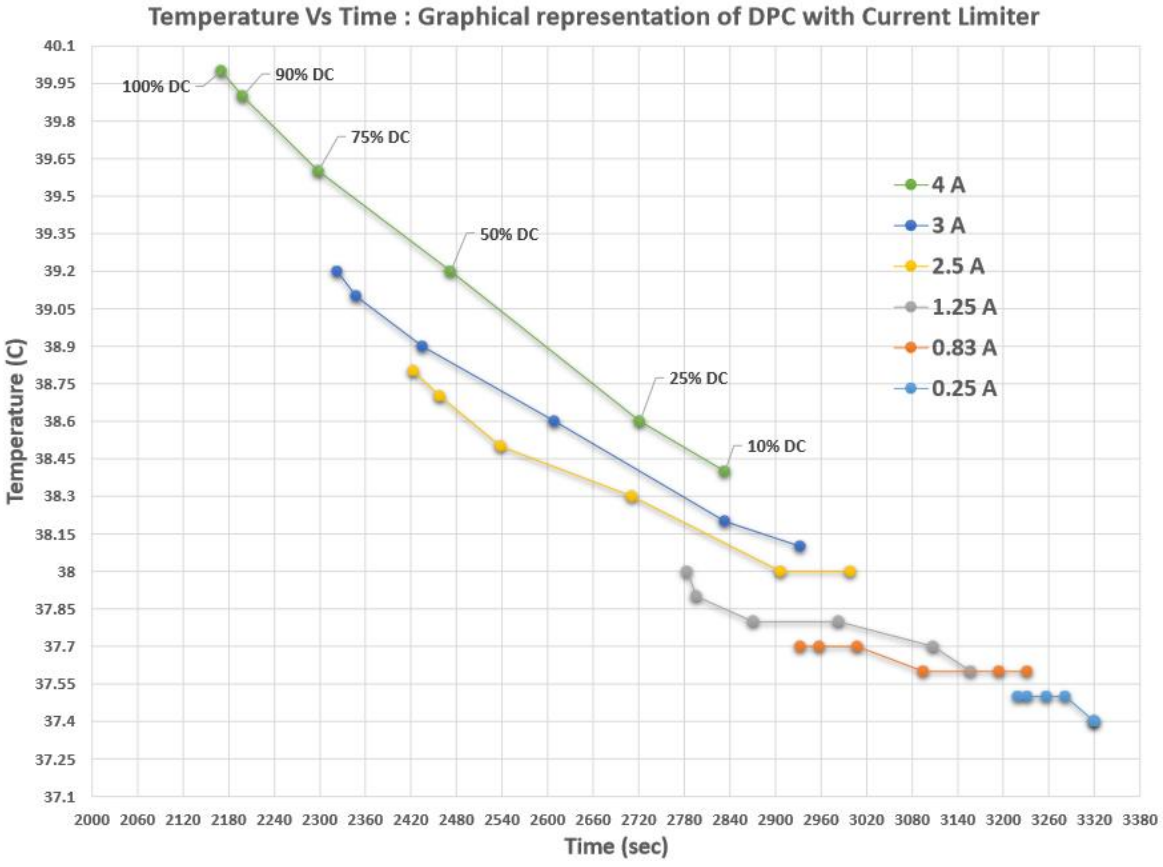

Figure 4.8: Temperature Vs. Time (Graphical Representation of Table 3)

As it is observed from Figure 4.7, also from the Figure 4.8 it can be said that Temperature is changing proportionally with the Duty Cycle with respect to any current and that the charging time is inversely proportional to the both Temperature and DC.

$$\textbf{Temperature } \alpha \textbf{ Duty Cycle}$$

$$\textbf{Charging Time } \alpha \ \frac{1}{\textbf{Duty Cycle}}$$

$$\textbf{Charging Time } \alpha \ \frac{1}{\textbf{Temperature}}$$

From Figure 4.7 and Figure 4.8, as we see the temperature and time change for any current amplitude follows a fixed trend (inversely proportional), it can be assumed that the optimal Temperature and charging Time for fast Battery charging will be any point in mid region of those Scatter linear graph. If we can find that point for the both graphs, then we can get the optimal temperature, required time to charge the battery and the current amplitude of our secondary pulse.

4.6 Finding optimal charging condition

As it is seen that we need to find the optimal point which lies in the mid region of the recorded data in Table 4.1 and Table 4.2, this point can be the nearest one of the Mean values of our recorded data. We can follow equation 16 for finding the mean of these values:

$$\textbf{Optimal Point} = \frac{\sum \textbf{Temperature} \times \textbf{Time}}{\textbf{n}} \qquad (16)$$

4.6.1 Optimal charging conditions of DPCS method without current limiter

Using the method discussed in Section 4.6, we found out the optimal result for Double Pulse Charging Method.

Here, we are recalling the Table 4.1 and doing calculation following the equation 16 where n = No. of data; which is for our case total 36 for all six currents (0.25 A, 0.83 A, 1.25 A, 2.5 A, 3 A & 4 A). Table 4.1 is split below for better visualization.

ON time		10%	25%	50%	75%	90%	100%
0.25A (0.1C)	**Time (sec)**	3331	3317	3281.25	3245.37	3216.21	3202.35
	Temp rise (°C)	38.3	38.3	38.3	38.3	38.3	38.3
	Time × Temp	127577.3	127041.1	125672.1	124297.9	123181.1	122650
0.83A (1/3C)	**Time (sec)**	3245.90	3188.01	3094.76	2994.39	2929.80	2915.46
	Temp rise(°C)	38.3	38.4	38.4	38.5	38.5	38.5
	Time × Temp	124318.08	122419.7	118839.1	115284.4	112797.4	112245.4
1.25A (0.5C)	**Time (sec)**	3173.65	3109.09	2972.85	2843.75	2764.85	2736.17
	Temp rise (°C)	38.4	38.5	38.5	38.7	38.8	38.8
	Time × Temp	121868.31	119700.3	114454.9	110053.1	107276.5	106163.6

Table 4.3: Finding the Optimal point using the proposed method (Data for 0.25A, 0.83A and 1.25A)

ON time		**10%**	**25%**	**50%**	**75%**	**90%**	**100%**
2.5A (0.1C)	**Time (sec)**	2945.19	2842.26	2636.49	2453.13	2361.82	2342.88
	Temp rise (°C)	39.1	39.2	39.5	39.8	40	40
	Time × Temp	115157.00	111416.90	104141.34	97634.73	94472.92	93715
3A (1/3C)	**Time (sec)**	2951.33	2822.22	2571.22	2370.39	2269.97	2241.28
	Temp rise (°C)	38.8	39	39.5	40	40.2	40.3
	Time × Temp	114511.41	110066.58	101563.03	94815.56	91252.91	90323.75
4A (0.5C)	**Time (sec)**	2836.23	2693.13	2420.58	2212.61	2115.02	2083.50
	Temp rise (°C)	39.2	39.5	40.2	40.7	41.1	41.2
	Time × Temp	111180.02	106378.56	97307.36	90053.20	86927.49	85840.08

Table 4.4: Finding the Optimal point using the proposed method (Data for rest of the currents 2.5A, 3A and 4A)

After the calculation using the data of both Table 4.3 & Table 4.4, it is found that,

Optimal Point (will be nearest to) = 109238.8327

From Table 4.3 and 4.4 it is seen that the mean value is closer to the data (green colored) found for 1.25 A secondary current amplitude with 75% duty cycle.

So, the found values in Double Pulse Charging Method (proposed method) are:

Optimal Temperature: 38.7° C (13.7° C temperature rise)

Charge Time: 2843.75 second

4.6.2 Optimal charging conditions of DPCS method with a current limiter

Similarly, like Table 5.4 here also the calculations are done for Table 4.1 Data. Following the same method of finding the optimal point, for 36 values (n) of all six currents (0.25 A, 0.83 A, 1.25 A, 2.5 A, 3 A & 4 A).

Table 4.2 is split below for better visualization.

ON time		**10%**	**25%**	**50%**	**75%**	**90%**	**100%**
0.25A (0.1C)	**Time (sec)**	3321.51	3319.62	3281.99	3257.24	3232.14	3219.73
	Temp rise (°C)	37.40	37.40	37.50	37.50	37.50	37.50
	Time × Temp	124224.51	124153.90	123074.51	122146.58	121205.40	120739.88
0.83A (1/3C)	**Time (sec)**	3232.14	3194.92	3095.20	3008.01	2958.16	2933.07
	Temp rise(°C)	37.60	37.60	37.60	37.70	37.70	37.70
	Time × Temp	121528.61	120129.10	116379.37	113401.86	111522.78	110576.63
1.25A (0.5C)	**Time (sec)**	3157.49	3107.78	2983.18	2871.00	2796.24	2783.58
	Temp rise (°C)	37.60	37.70	37.80	37.80	37.90	38.00
	Time × Temp	118721.77	117163.16	112764.17	108523.65	105977.61	105776.04

Table 4.5: Finding the Optimal point using the proposed method (with a CL) (Data for 0.25A, 0.83A and 1.25A)

ON time		10%	25%	50%	75%	90%	100%
2.5A (0.1C)	**Time (sec)**	2999.32	2906.91	2711.154	2538.42	2458.01	2423.41
	Temp rise (°C)	38.00	38.00	38.30	38.50	38.70	38.80
	Time × Temp	113974.12	110462.69	103837.20	97729.21	95124.83	94028.46
3A (1/3C)	**Time (sec)**	2932.98	2833.65	2609.27	2435.05	2347.97	2322.93
	Temp rise(°C)	38.10	38.20	38.60	38.90	39.10	39.20
	Time × Temp	111746.69	108245.47	100717.63	94723.56	91805.55	91058.97
4A (0.5C)	**Time (sec)**	2833.61	2721.61	2472.40	2298.02	2198.38	2170.21
	Temp rise (°C)	38.40	38.60	39.20	39.60	39.90	40.00
	Time × Temp	108810.59	105054.26	96918.04	91001.67	87715.28	86808.52

Table 4.6: Finding the Optimal point using the proposed method (with a CL) (Data for rest of the currents 2.5A, 3A and 4A)

After the calculation using the data of both Table 4.5 & Table 4.6, it is found that,

Optimal Point (will be nearest to) = 104409.929

From Table 4.5 and 4.6, it is seen that the mean value is closer to the data (green colored) found for 2.5 A secondary current amplitude with 50% duty cycle.

So, the found values in DPC Method with an extra current limiter are:

Optimal Temperature: 38.3° C (13.3° C temperature rise)

Charge Time: 2711.154 second

So, here we are proposing 2 ways of DPC Method. One without the Extra CL and other one with an Extra CL. And we have found from our simulation that without CL we are getting comparatively higher charge time (around 100s higher) and temperature (0.4° C higher) than the method with an extra CL. For the DPC Method with an extra current limiter we are injecting Secondary Current amplitude of 2.5A with 50% duty cycle to gain so and for the DPC Method without an extra current limiter this current amplitude of 1.25A with 75% duty cycle. As battery's internal polarization plays a vital role in determining battery life, these 2 methods have almost similar trade off.

4.7 Comparison and improvements over previous methods

In this section, a comparison is presented in table 4.7 for the CCCV method, polarization method, the SPCS method and the proposed methods. The experiment results show that the proposed charge method achieves the fast charging speed within operating temperature. This is especially suitable for the charge for EV or PHEV from 0% SOC to 80% SOC **[14].**

No.	Charge Mode	Temperature Rise (°C)	0%-80% Charge Time(s)
1	Proposed (Double Pulse Charging)	13.7	2843.75
2	Proposed (Double Pulse Charging with an Extra CL)	13.3	2711.154
3	SPC Method	13.3	3373
4.	Polarization Method	12	4079
5.	CCCV at 2C	10	4075

Table 4.7: Comparison of Evaluation results **[14]**

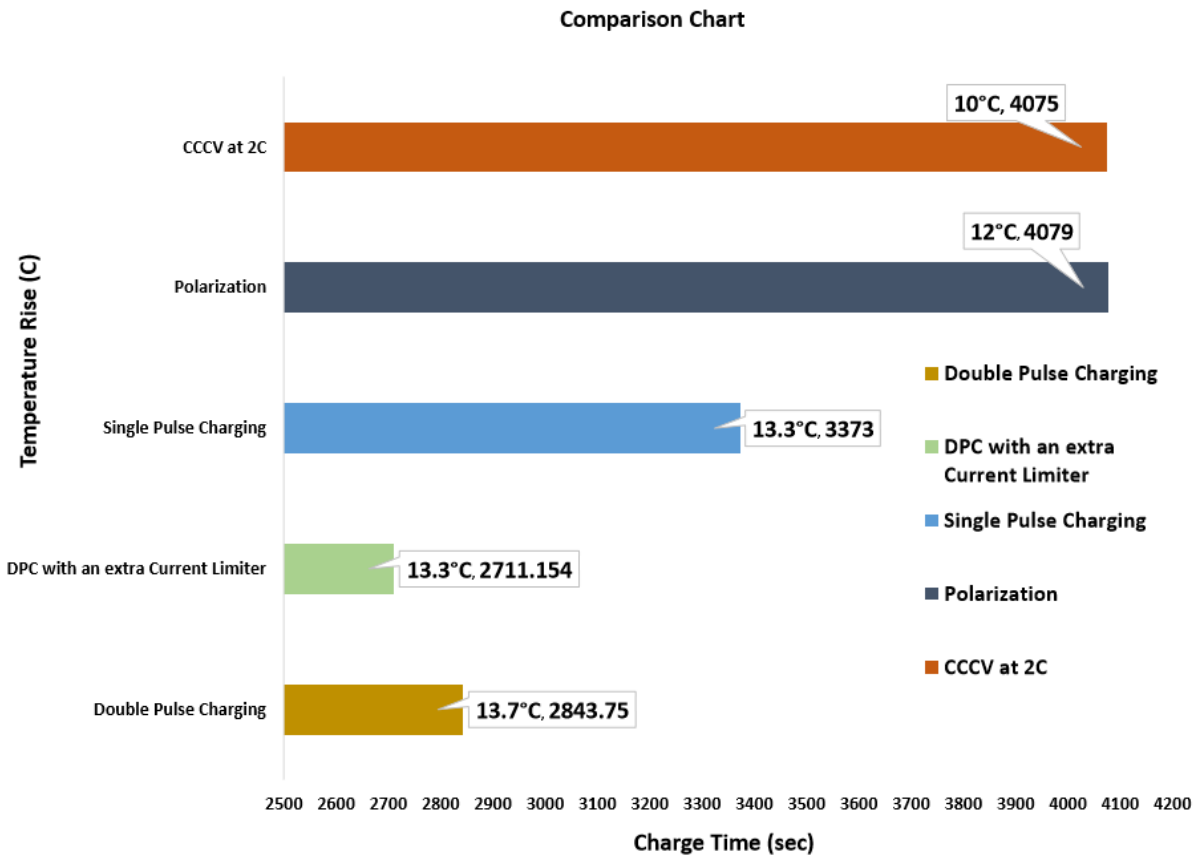

Figure 4. 9: Graphical representation of the comparison among proposed methods and other charging methods (Temperature Rise Vs. Charge Time Graph) **[14]**

So, from Figure 4.9 it is clearly visible that we have been successful to reduce the charge time of the Battery maintaining the decent Temperature rise while at the same time been able to faster charge the battery by implementing the Double Pulse Charging Method.

The battery charging using the proposed method (DPCS Method) has been successfully proved to be 10 minutes faster than SPCS, while being 23 minutes faster than the CCCV and polarization methods. At the same time, the temperature rise does not exceed 40 degrees, which is considered a safe charging region for the battery.

4.8 Conclusion

To sum up, our contribution of integrating the double pulse technique alongside the SPCS method has proven to be highly beneficial as observed in this chapter. By manipulating the ON period as well as varying the current amplitude of the secondary pulse we were able to observe various charging times and temperature rises for each case. Furthermore, limiting the current amplitude of the primary current allowed us to not only lower the temperature, but also use a higher secondary current amplitude thereby allowing for a higher charging speed. Altogether this has proved to be a much faster charging system than SPCS method by 19.6 percent for the same temperature rise, while being 33 percent faster than traditional methods with a higher temperature rise. Regardless, this method can be considered to be a much better solution to the long charging time while keeping the temperature within bounds.

Chapter 5: Conclusion & Future works

5.1 Conclusion

Lithium-ion battery can be charged by various techniques and each technique has their own limitations. The conventional CC-CV technique almost used in every commercial charger is effective but not efficient for Fast Charging Method. For faster charging, many papers have attempted various methods of fast charging. In this paper, we came up with an optimal technique to minimize the charging time, keeping the temperature rise in an optimal range. The Double Pulse Charging Method (with or without an extra Current Limiter) is implemented here combining the concept of Single Pulse Charging using Polarization Method by implementing a variable duty cycle and variable frequency searching technique, thereby achieving a better result.

A literature review was conducted which analyzed different possibilities for modeling and the previous research into pulse charging. From the literature review, it became apparent that one of the challenges with this type of research is the significant differences that exist between the different types of battery chemistries, even amongst lithium ion cells. The review of pulse charging papers suggested that faster charging could be achieved through Pulse Charging Method.

The objective of this thesis was to analyze the effects of double pulse charging via Simulink, implemented into the model to appropriately reflect pulsed charging operation to improve the charging time, and a significant difference was realized between Single Pulse Charging and Double Pulse Charging Method.

The double pulse method is an efficient choice, since the battery is fed by two different current amplitudes followed by resting periods, thus allowing a decrease of the charging time in a safe environment with a very small temperature rise within the optimal boundary.

This paper has made some effective discovery in Fast Charging Methods. Two methods (DPC & DPC with an extra CL) are proposed here and the results compared to Single pulse method are showing that for DPC without a current limiter the charging time has improved by 15.7% with only 3% Temperature rise than SPC while for DPC using a Current Limiter the charging time has improved by 19.6% with same amount of Temperature rise as SPC. Furthermore, comparing to the traditional CCCV method, it can be observed that the improvement of charging speed is about 30 percent with a temperature rise by 37 percent for DPC without a current limiter, while for a DPC using a current limiter, the charging time is improved by 33.4 percent, with a temperature rise of 33 percent.

Therefore, we can conclude that the DPC using current limiter method is the most optimal and least harmful method to optimally charge a Li-Ion battery in much less time while keeping within the optimal Temperature range (25°- 40°).

5.2 Future works

This research is not limited to a single model battery, but future work can be done to establish this universal charging method for all types of batteries. In addition, for different batteries the simulation approach can also be used to predict the effect of this algorithm. Effects on series and parallel battery combinations using this charging method can be considered, and the lifespan of such batteries after multiple charging cycles can be a great opportunity for future work. Together, there is a strong expectation that one of the strongest methods of charging li-ion batteries will lead the world to a greener and brighter future.

References

[1] H. Venkatasetty and Y. Jeong, “Recent advances in lithium-ion and lithium-polymer batteries,” Seventeenth Annual Battery Conference on Applications and Advances. Proceedings of Conference (Cat. No.02TH8576).

[2] X. Yang, G. Zhang, S. Ge and C. Wang, "Fast charging of lithium-ion batteries at all temperatures", *Proceedings of the National Academy of Sciences*, vol. 115, no. 28, pp. 7266-7271, 2018.

[3] T. Waldmann, M. Kasper and M. Wohlfahrt-Mehrens, "Optimization of Charging Strategy by Prevention of Lithium Deposition on Anodes in high-energy Lithium-ion Batteries – Electrochemical Experiments", *Electrochimica Acta*, vol. 178, pp. 525-532, 2015.

[4] T. Waldmann, M. Wilka, M. Kasper, M. Fleischhammer and M. Wohlfahrt-Mehrens, "Temperature dependent ageing mechanisms in Lithium-ion batteries – A Post-Mortem study", *Journal of Power Sources*, vol. 262, pp. 129-135, 2014.

[5] C. Mao, R. Ruther, J. Li, Z. Du and I. Belharouak, "Identifying the limiting electrode in lithium ion batteries for extreme fast charging", *Electrochemistry Communications*, vol. 97, pp.37-41,2018.

[6] G. Trentadue, A. Lucas, M. Otura, K. Pliakostathis, M. Zanni and H. Scholz, "Evaluation of Fast Charging Efficiency under Extreme Temperatures", *Energies*, vol. 11, no. 8, p. 1937, 2018.

[7] G. Pistoia, *Battery operated devices and systems*. Amsterdam: Elsevier, 2009.

[8] D. Duong, “DFT calculations for cathode materials of rechargeable Li-ion batteries,” no. June, 2016, doi: 10.13140/RG.2.1.2641.1120.

[9] T. Crompton, *Battery reference book*. Oxford: Newnes, 2000.

[10] Ponnuchamy, Veerapandian. (2015), “Towards a Better Understanding of Lithium Ion Local Environment in Pure, Binary and Ternary Mixtures of Carbonate Solvents: A Numerical Approach.”

[11] M. Morris, “Comparison of Rechargeable Battery Technologies,” *ASME Early Career Tech. J.*, 2012.

[12] G. J. May, A. Davidson, and B. Monahov, “Lead batteries for utility energy storage: A review,” Journal of Energy Storage. 2018, doi: 10.1016/j.est.2017.11.008.

[13] M. Morris, “Comparison of Rechargeable Battery Technologies,” *ASME Early Career Tech. J.*, 2012.

[14] M. Yin, J. Cho and D. Park, "Pulse-Based Fast Battery IoT Charger Using Dynamic Frequency and Duty Control Techniques Based on Multi-Sensing of Polarization Curve", *Energies*, vol. 9, no. 3, p. 209, 2016.

[15] Yin, M.D.; Youn, J.; Park, D.; Cho, J, “Efficient Frequency and Duty Cycle Control Method for Fast Pulse-Charging of Distributed Battery Packs by Sharing Cell Status”. In Proceedings of the International Workshop on Ubiquitous Wireless Sensor, Beijing, China, 10–14 August 2015; pp. 40–45.

[16] N. Keskin and H. Liu, "Double-pulse charge technique for wireless and mobile devices", *Analog Integrated Circuits and Signal Processing*, vol. 86, no. 2, pp. 299-305, 2015.

[17] J. Jiang, Q. Liu, C. Zhang and W. Zhang, "Evaluation of Acceptable Charging Current of Power Li-Ion Batteries Based on Polarization Characteristics", *IEEE Transactions on Industrial Electronics*, vol. 61, no. 12, pp. 6844-6851, 2014.

[18] S. Zhang, K. Xu, and T. Jow, “Study of the charging process of a LiCoO2-based Li-ion battery,” *Journal of Power Sources*, vol. 160, no. 2, pp. 1349–1354, 2006.

[19] A. B. Khan, V.-L. Pham, T.-T. Nguyen, and W. Choi, “Multistage constant-current charging method for Li-Ion batteries,” *2016 IEEE Transportation Electrification Conference and Expo, Asia-Pacific (ITEC Asia-Pacific)*, 2016.

[20] P. Notten, J. O. H. Veld, and J. V. Beek, “Boost charging Li-ion batteries: A challenging new charging concept,” *Journal of Power Sources*, vol. 145, no. 1, pp. 89–94, 2005.

[21] J. Li, E. Murphy, J. Winnick, and P. A. Kohl, “The effects of pulse charging on cycling characteristics of commercial lithium-ion batteries,” *Journal of Power Sources*, vol. 102, no. 1-2, pp. 302–309, 2001.

[22] A. Tomaszewska, Z. Chu, X. Feng, S. O'Kane, X. Liu, J. Chen, C. Ji, E. Endler, R. Li, L. Liu, Y. Li, S. Zheng, S. Vetterlein, M. Gao, J. Du, M. Parkes, M. Ouyang, M. Marinescu, and B. Wu, “Lithium-ion battery fast charging: A review,” *eTransportation*, 16-Aug-2019.

[23] M. He, “Testing, Characterization, and Thermal Analysis of Lithium-Ion Batteries Toward Battery Pack Design for Ultra-Fast Charging,” *Handle Proxy*, 01-Jan-1970. [Online]. Available: http://hdl.handle.net/11375/24158.

[24] Johnson Matthey Battery Systems, “Guide to Batteries,” 2017. M.A.Sc. Thesis – M. He; McMaster University – Mechanical Engineering

[25] Haizhou, Z. (2017). Modeling of Lithium-ion Battery for Charging/Discharging Characteristics Based on Circuit Model. *International Journal Of Online Engineering (Ijoe)*, *13*(06), 86. doi: 10.3991/ijoe.v13i06.6799

[26] R. C. V. Dongen, “Li-Ion Charger for Implantable Devices - Selection of optimal charge algorithm and implementation,” *Semantic Scholar*, 07-Dec-2012. [Online]. Available: https://www.semanticscholar.org/paper/Li-Ion-Charger-for-Implantable-Devices-Selection-of-Dongen/8268994a29ffe8e9b07ea2fbcfd03190c3682f3b.

[27] T. Huria, M. Ceraolo, J. Gazzarri, and R. Jackey, “High fidelity electrical model with thermal dependence for characterization and simulation of high power lithium battery cells,” *2012 IEEE International Electric Vehicle Conference*, 2012.

[28] Rajanna, B. and Kiran Kumar, M., 2020. Comparison of one and two time constant models for lithium ion battery. *International Journal of Electrical and Computer Engineering (IJECE)*, 10(1), p.670.